ELECTRON TECHNOLOGY
ISSN 1897-2381
http://www.ite.waw.pl/etij/
Internet Journal

SURFACE TREATMENTS OF GaSb AND RELATED MATERIALS FOR THE PROCESSING OF MID-INFRARED SEMICONDUCTOR DEVICES

E. PAPIS-POLAKOWSKA

Institute of Electron Technology, al. Lotników 32/46, 02-668 Warszawa, Poland

Received January 30, 2006; accepted June 23, 2006; published July 18, 2006

CONTENTS

ABSTRACT

Various chemical treatments of GaSb and related compounds has been studied with the aim to develop procedures of polishing of GaSb substrates, preparation of their surfaces for deposition of metal and dielectric films, for liquid phase epitaxial growth, and finally fabrication of passivating coatings on surfaces of GaSb and its alloys. A broad spectrum of surface characterisation techniques has been used to analyse morphology of the surface and its chemical composition after each of the treatments applied. This allowed us to elaborate a complete set of technological procedures necessary for the fabrication of the efficient GaSb-based photo- and light emitting diodes operating in the mid-infrared wavelength range.

1. Introduction

GaSb-based semiconductor alloys are well recognised for their potential applications in mid-infrared optoelectronics and thermophotovoltaics. The implementation of these materials, however, has been hampered by problems with reproducible control of their surface properties. In this work we have studied various chemical treatments of GaSb with the aim to develop procedures of polishing of GaSb substrates, preparation of their surfaces for deposition of metal and dielectric films, for liquid phase epitaxial growth, and finally fabrication of passivating coatings on surfaces of GaSb and its alloys. After each of these steps the surface was examined with the use of optical microscopy, scanning electron microscopy, atomic force microscopy, transmission electron microscopy, spectroscopic ellipsometry and X-ray photoelectron spectroscopy to analyse morphology of the surface, its chemical composition and to check for presence of surface defects.

The paper is organised as follows: first we review some basic structural and physicochemical properties of GaSb surfaces that must be taken into account when designing processing of GaSb-based optoelectronic devices. In particular, we point out a complicated structure of GaSb surfaces and their high chemical reactivity. Next, we present details of experimental methods applied for surface treatment and complementary microanalytical techniques used for complete characterisation of treated surfaces. The main part of the paper presents experimental results on polishing of GaSb substrates, etching of GaSb by wet and dry etching techniques and fabrication of patterns on GaSb wafers by photolithography and etching. Finally, we present results of our studies on

chemical and electrochemical passivation of GaSb, InGaAsSb and AlGaAsSb surfaces.

1.1. Structural and physicochemical properties of GaSb surfaces

Gallium antimonide and related compounds crystallise in the zinc-blende structure. This structure, illustrated in Fig. 1, can be considered as two interpenetrating face-centered-cubic lattices with group III and group V atoms located on different sublattices. The lattice constants and energy band

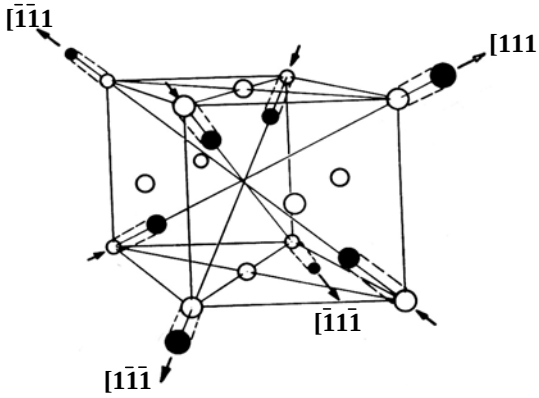

Fig. 1. The zinc-blende structure of the III-V semiconductors.

gaps of representative compounds are given in Table 1. Figure 2 shows band gap energy and

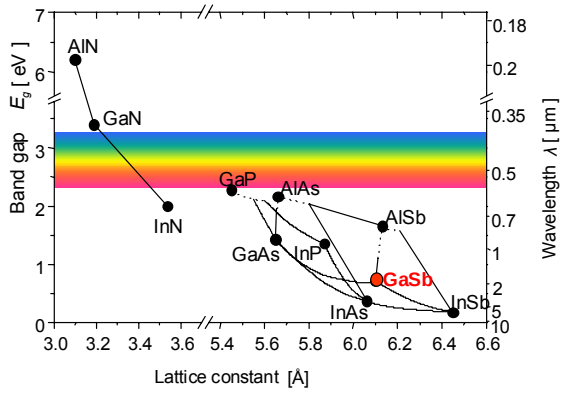

Fig. 2. Band gap and respective wavelength as a function of lattice constant for III-V semiconductors.

respective wavelength as a function of lattice constant for III-V semiconductors.

Table 1. Lattice constants and band gap for selected III-V compound semiconductors.

Semiconductor compound	Lattice constant a^* [Å]	Band gap E_g^* [eV]
AlSb	6.1355	1.63
GaSb	6.0955	0.72
InAs	6.0585	0.35
InSb	6.4788	0.16

* at $T = 300$ K

In contrast to elemental semiconductors with pure covalent bonding, the bonds in the zinc-blende compounds are of mixed covalent-ionic type. For example, the ionicity of GaSb is 0.33 that indicates some charge transfer between Ga and Sb atoms.

The ionic contribution to the bonding in III-V semiconductors manifests itself in their cleavage behaviour. Crystals cleave along the non-polar (110) plane, although the least numbers of bonds would be broken by cleavage along (111) planes. This is why covalent Si and Ge crystals cleave along this plane. The ideal structures of the (001), (110) and (111) surfaces are illustrated in Fig. 3. The polar (001) and (111) surfaces are composed of layers of all group III or all group V elements, whereas in the ideal case the (110) surface consists of equal number of each of the constituent atoms. Some of the non-polar cleaved (110) surfaces have been thoroughly studied by low-energy electron diffraction [1]. In all studies the symmetry of the surface unit mesh is that expected for a truncated bulk solid. That is, there is no re-construction of surface that could lead to unexpected diffraction pattern. There are several reasons, however, for believing that the surface atoms are relaxed from their ideal bulk positions, adopting a configuration illustrated in Fig. 4 [2].

Both (001) and (111) surfaces are polar due to the alternate arrangement of the anion and cation layers parallel to the surface, so that the ideal surface may consist of all anions or all cations. In practice these surfaces are rarely ideal and display numerous reconstructed forms, which depend on the method of preparation and the chemical composition of the surface.

Real surfaces modified by technological processes exhibit a surface damage region (particularly after cutting, smoothing or mechanical polishing) containing many defects as steps, vacancies, stress, contaminants and native oxides. Impurities on semiconductor surface may be physically or chemically absorbed gas, metal ions, organic material or their combination, and stable chemical compounds. Metallic contamination usually comes from chemical agents, whereas photoresists or organic solvents may be a source of organic pollution. Exposure of semiconductor surface to atmosphere activates reaction with oxygen or steam and causes formation of a native oxide layer.

GaSb surface is much more reactive than that of GaAs or InP and quickly oxidises under atmospheric conditions forming an oxide layer that is neither self--limiting, stable nor abrupt [3]. Chemical reactivity of antimonides distinguishes them such a distinct category of materials [4–9].

The irreversible nature of the reactions suggests that oxygen atoms, rather than molecules, are ultimately involved in the chemical bonding. The value of 3 – 4 oxygen atoms per surface atom is too high to be explained plausibly by the chemisorption

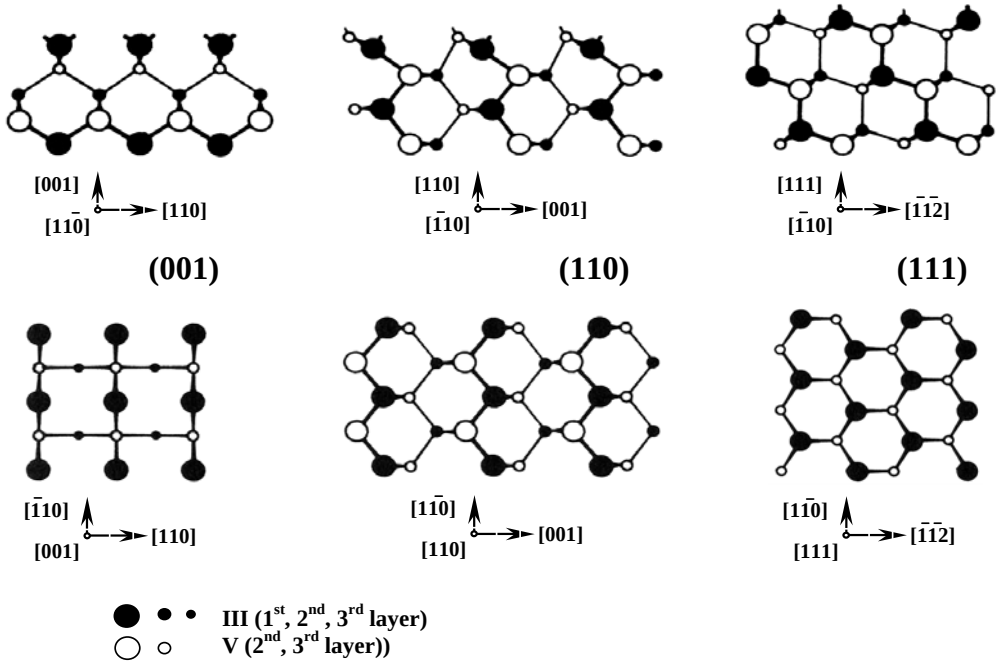

Fig. 3. The structure of (001), (110), and (111) surfaces of a zinc-blende compound semiconductor [1].

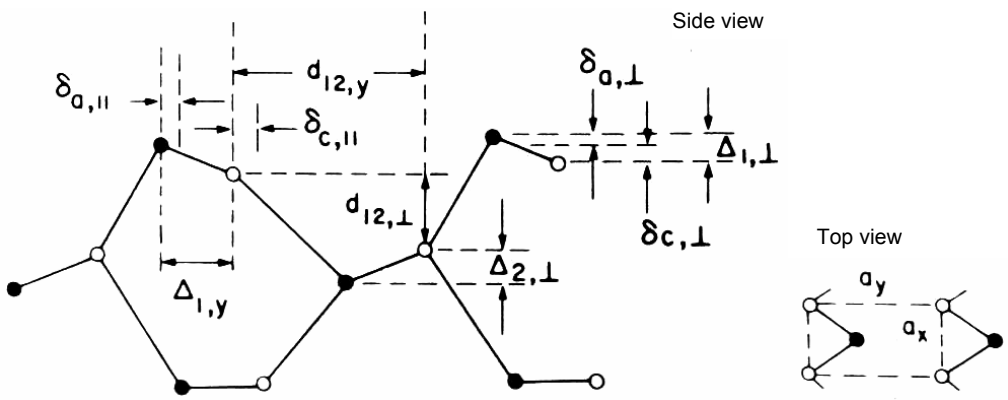

Fig. 4. The relaxed (110) surface of III-V compound semiconductor [2].

of oxygen on the original surface atoms alone, so that additional atoms probably take part in the formation of the intermediate structures. One moves, therefore, from the usual concept of chemisorption, where the structure of the adsorbed layer is determined primarily by the structure of the underlying surface, to the concept of complex formation, in which the film can have a chemical and structural identity of its own.

Figure 5 shows the oxidation rate of III-V semiconductor compounds at room temperature. The uptake of oxygen by each sample is normalised to unit surface area being determined by krypton adsorption at – 195°C. It is seen that group III antimonides oxidise much faster than other III-V compounds. This distinction has a parallel in the classical oxygen chemistry of the group V elements. While antimony is octahedrally co-ordinated by oxygen, arsenic and phosphorous are tetrahedrally co-ordinated in their oxygen compounds. No such distinction exists among the group III elements where octahedral coordination is generally observed.

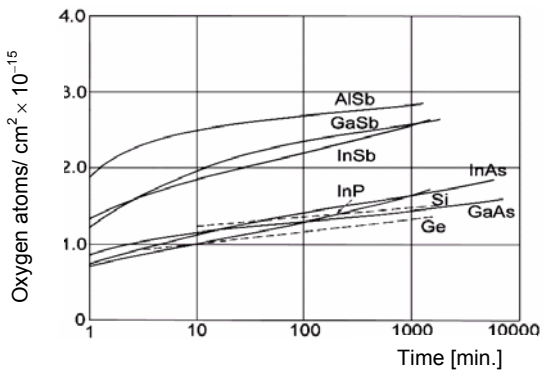

Fig. 5. The rates of oxygen sorption on III-V semiconductor surfaces at $T = 26.2$°C [4].

The composition of the oxide layers is determined by kinetic factors, such as rates of reaction, diffusion, dissolution, and evaporation and thermodynamics, which predicts the equilibrium oxidation products. Some important information on the equilibrium in the oxygen-III-V system provides respective ternary phase diagram (Fig. 6). If elements or compounds are

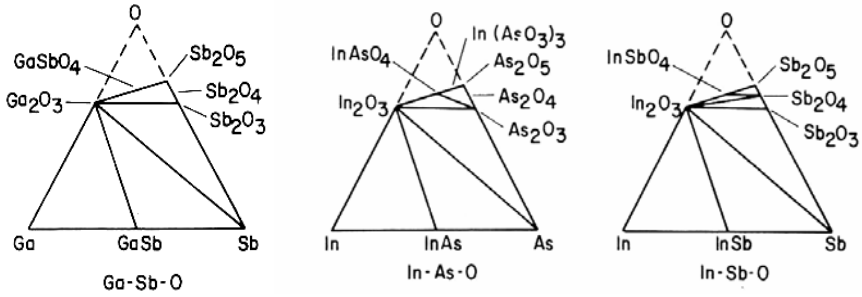

Fig. 6. Phase diagrams of the GaSb, InAs and InSb with oxygen.

connected by a line (called tie line) then no reaction is possible between these two. For example, GaSb does not react with O to form other compounds.

Conversely, if two elements or compounds are not connected by a tie line, then a reaction can occur. The products of such a reaction are those at each end of the tie lines cut by a line connecting the two reactants.

Investigations on kinetics of reaction between GaSb surface and oxygen showed that it takes a course in two steps [10]:

$$2GaSb + 3O_2 \rightarrow Ga_2O_3 + Sb_2O_3,$$
$$2GaSb + Sb_2O_3 \rightarrow Ga_2O_3 + 4Sb.$$

Table 2 summarises the equilibrium interface composition and the composition observed after different types of oxide growth. Table 3 lists some properties of various III-V oxides.

Table 2. Oxidation of III-V compounds surface [11].

III-V comp.	Equilibrium	Air/ chemical oxide	Thermal oxide	Anodic oxide
GaSb	$Ga_2O_3 + Sb$		$Ga_2O_3 + Sb$	$Ga_2O_3 + Sb_2O$
InAs	$In_2O_3 + As$		$In_2O_3 + As$ $In_2O_3 + As_2O_3$	$In_2O_3 + As_2O_3$
InSb	$In_2O_3 + Sb$	$In_2O_3 + Sb_2O_3$	$In_2O_3 + Sb$	$In_2O_3 + Sb_2O_3$

Table 3. Properties of III-V oxides [11].

Oxide	Structure	Melting point [°C]	Density [g/cm^3]	Refractive index			E_g [eV]	ΔG_F [kcal/mol]	ΔH_F [cal/mol]	C_p [cal/mol]
				N_α	N_β	N_γ				
β-Ga_2O_3	Monoclinic	1715	5.95	1.93	–	–	4.7	–238.6	–260.3	22.0
$GaSbO_4$	Tetragonal	–	6.57	–	–	–	–	–218.4	–246.2	–
$InSbO_4$	Orthorhombic	–	–	–	–	–	–	–198.4	–226.7	–
As_2O_3	Monoclinic	313	4.15	2.01	1.92	1.87	4.0	–137.91	–156.5	22.86
As_2O_5	Hexagonal	> 827	4.09	–	–	–	–	–187.0	–221.05	–
Sb_2O_3	Cubic	655	5.2	–	2.08	–	6.72	–151.5	–172.1	27.85
	Orthorhombic	–	5.67	2.35	2.35	2.18	–	–149.7	–169.3	24.23

It is worth noticing that an abrupt layer of elemental Sb may form at the oxide/GaSb interface giving rise to unwanted conduction paths parallel to the interface (large surface leakage) and high surface state density [12].

Different structure of semiconductor surface than that of semiconductor bulk has a fundamental influence on the electrical properties of semiconductor surface. It leads to the generation of electronic states, so called surface and resonance states, which results in Fermi level pinning on semiconductor surface. It is important to emphasise that the Fermi level pinning may be caused by as little as $10^{12} \div 10^{13}$ cm^{-2} density of surface states. Both chemisorption and chemical reactions may lead to a modification of surface states and generation of new donor and acceptor states in the energy gap. These states, in turn, may lead to band bending and a surface space-charge layer. Again, a density of surface states of around 10^{12} cm^{-2} may be sufficient for appreciable effects, so that an adsorbate surface coverage of $0.1 \div 1\%$ of a monolayer can have significant affects on the electronic properties. In consequence, surface properties such as surface conductivity, surface recombination velocity, mobility of carriers and etching rate significant depend on state of the surface.

Study of the preparation methods of semiconductor surfaces that are free of damage, contamination and native oxides is necessary for reproducible and efficient control of surface properties. For research purposes such surfaces are formed by cleaving, annealing in high vacuum and by epitaxial growth methods (first of all by MBE technique). In device technology practice contact with atmosphere is unavoidable and surface preparation takes place most often by etching process.

1.2. Chemical treatment of GaSb surfaces

1.2.1. Etching processes

The choice of etching process and of proper chemical agent (solution or gas) depends on chemical composition of etched material and on intended result of surface treatment. The aim of etching process may be:

- removal of surface layer damaged as a result of surface cutting, polishing or thinning processes;
- creation of clean surface, free of oxides and residual contamination;
- revealing of low index planes and defects;
- etching of surface patterns and the control of surface recombination velocity.

In this context the terminology distinguishes:

- polishing etching process – homogenous removal of semiconductor surface without surface damage;
- preferential etching – the process that reveals crystallographic planes;
- non-preferential etching – the process generating pits and revealing dislocations;
- anisotropic etching in which horizontal etching rate significantly surpasses vertical one; $v_h >> v_v$ (Fig. 7b);
- isotropic etching, in which anisotropy factor $A = 1 - v_h/v_v$ has a value of about one (Fig. 7c);
- selective etching, in which etching rate of overlying layer material significantly surpasses the etching rate of the material lying below (Fig. 8);
- non-selective etching, in which selectivity factor $S_{AB} = v_A/v_B$ has a value of about.

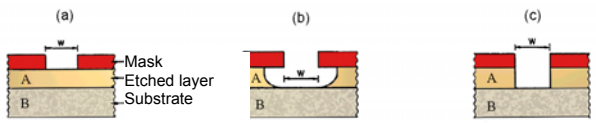

Fig. 7. Pattern etching in material A: a) pattern in mask material, b) anisotropic etching, c) isotropic etching.

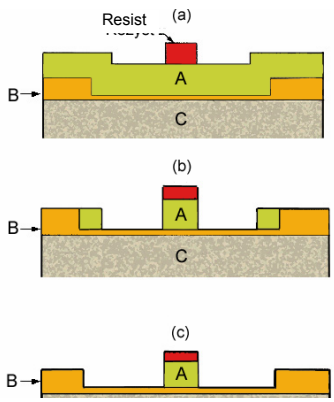

Fig. 8. Selective etching in material A towards to B and C materials.

The ease with which atoms are removed from the surface depends on their binding energy, the number of bonds between atoms and surface and the kind of atom being removed. The covalent bonding of the III-V compounds requires the presence of an oxidising agent to break the bonds. However, a few of the compounds have enough ionic character of the bonds to be attacked by HCl. The oxidising agent may be chosen from the redox table and HNO_3, H_2O_2, Fe^{3+}, or MnO_4^- may be taken into consideration as oxidising agents. In most cases complexing agents must also be added to the oxidising agent to help forming ions stable in the etchant. The acid etchants such as HF, HCl and H_2SO_4 may be used to remove surface oxides.

Chemical etching

Chemical etchants for GaSb and related compounds are given in Tables 4–6. Note that InSb, GaSb, and their solid solution require an oxidising agent. Most often HNO_3 and H_2O_2 are used for this purpose. Only AlSb has sufficiently ionic character to not require oxidant and to react with HCl. Optimisation of solution composition is necessary for control of reaction method and products. For example, if the ratio of HNO_3 to HCl is very large, insoluble antimony tri- or pentoxide forms while all other ratios yield soluble antimony chlorides. For strong acidic solutions addition of complexing agents such as tartaric or citric acid is necessary for prevent solution from total dissociation. Thus, ratios of HNO_3 to organic acids must favour the organic acids. HNO_3 is at the same time oxidising and etching agents because it oxidises III-V surfaces and etches III – V oxides (Ga_2O_3 and In_2O_3), simultaneously leaving the group V oxides (Sb_2O_3 and As_2O_3).

Table 4. Chemical etchants for GaSb.

Etchant		Type of etching	Ref.
Composition	Ratio		
HF + HNO_3 + + CH_3COOH	6 + 2 + 1	Removing of native oxides	13
HNO_3 + HF + + CH_3COOH Br_2 + methanol	1 + 10 + 15	Polishing	14
HCl + H_2O_2 + NaK	0.7 + 7 + 25	Polishing	14
HNO_3 + citric acid	1 + 3	Dislocations on (111)	15
CH_3COOH + HNO_3 + + HF	20 + 9 + 1	Dislocations on (111)	13
CH_3COOH + HNO_3 + + HF	40 + 18 + 2	Mesa etching	16
HF + HNO_3 + H_2O_2	1 + 1 + 1	Orientation (001)	17

In the H_2SO_4-H_2O_2-H_2O system H_2O_2 oxidises GaSb surface while H_2SO_4 etches oxides created. H_2O_2 is neutralizator, which reduces the rate of etching and creates oxide layer on etched surface. The thickness of this oxide layer depends on pH of the solution, which is determinated by the H_2SO_4:H_2O_2 ratio.

Dry etching

There is a very small number of literature reports on dry etching of group III antimonides. Most often Reactive Ion Etching (RIE) has been applied using

CCl_4, CCl_2F_2/O_2, CH_4/H_2 or C_2H_6/H_2 plasma [23–25], recently also Cl_2/Ar [26, 27]. Few studies have also been published on electron cyclotron resonance (ECR) plasma etching in either Cl_2/Ar or BCl_3/Ar [28], [29] and on chemically assisted ion beam etching (CAIBE) with an Ar^+/I or Ar/Cl_2 [30].

Table 5. Chemical etchants for InSb.

Etchant		Type of etching	Ref.
Composition	Ratio		
$HF + HNO_3$	1 + 1	Polishing	18
$HF + HNO_3 +$ $+ CH_3COOH$	1 + 2 + 1	Polishing	19
HNO_3 + lactic acid	1 + 10	Polishing	20
$HF + HNO_3 + H_2O$	1 + 1 + 4	Orientation (001)	17
$HF+ HNO_3 CH_3COOH$	1 + 2 + 5	Removing of native oxides	21
$HF + HNO_3 + H_2O$	5 + 5 + 2	Dislocations on (110) and (100)	22

Table 6. Chemical etchants for AlSb.

Etchant		Type of etching	Ref.
Composition	Ratio		
$HNO_3 + HF +$ $+ CH_3COOH$	3 + 2 + 5	Polishing	22
$HNO_3 + HF +$ $CH_3COOH + Br_2$	25 + 15 + 15 + 3	Dislocations on (100)	17
$HNO_3 + HF + H_2O$	5 + 5 + 1	Masa etching	17

Electrolytic etching

In this process etched material is placed on the anode, which together with an inert cathode (usually Pt) is dipped in a suitable electrolyte. The electrolyte must have enough electrical conductivity and products of reaction must be soluble in the electrolyte. Some common electrolytes and the typical conditions of their use are given in Table 7. Generally, when HNO_3 is used as oxidising agent the etching process is controlled by reaction, while diffusion controls the process in H_2O_2 – containing electrolytes.

Table 7. Electrolytic etching for III-V semiconductor compounds.

Com-pound	Composition of etching mixture	Current density [A/cm^2]	Type of etching	Ref.
InSb	(HNO_3+ ethylene glycol) = (1 + 8) + few drops of HF	0.1 – 1	Polishing	17
InSb	($HClO_4 + H_2O$ + acetic anhydride) = = (10 + 2 + 40); T = 5°C	0.05	Polishing	31
GaSb	(Perchloric acid + acetic acid) = (1 + 4)	–	Polishing	32
InAs	(Perchloric acid + acetic acid) = (1 + 4)	–	Polishing	33

1.2.2. Surface passivation

High surface state densities, surface Fermi level pinning and a residual oxide layer on the surface are the common problems of all III-V semiconductors. These phenomena have a negative effect on the efficiency of many micro- and optoelectronic devices. To eliminate their undesirable influence on device properties, the direction called "surface passivation" is being actively developed. Ideal surface passivation process must prevent a semiconductor from reaction with the atmosphere during the entire lifetime of semiconductor device (chemical passivation). Then it must remove interfacial states from the band gap and/or prevent their formation (electrical passivation). Finally, it must form the effective barrier for possible transfer of electrons from semiconductor surface to the passivating layer. The term "passivation" signifies that as the result of the treatment a semiconductor surface becomes less chemically active, a number of recombination centres on the surface is reduced and/or these centres themselves become less active.

Research on passivation of III-V semiconductor surfaces follows two main directions. The first group of techniques makes use of deposition on the surface of relatively thick insulator layers. Their thickness range from several tens of nanometers to several micrometers. Then a semiconductor-insulator heterojunction is formed, properties of which depend on the initial density of interface states and surface treatment (surface pretreatment and heterojunction preparation) applied. These processes include passivation by the native oxide and by oxides obtained by thermal, plasma or anodic oxidation. The other direction is modification of the surface by the group V and VI atoms, which change its electronic structure. This method is often used as the surface pretreatment. It is worth noticing that silicon native oxide SiO_2 acts as ideal surface passivation. Unfortunately, for III-V compound semiconductors analogous surface passivation by native oxide does not work so well. The coatings formed by anodic oxidation are one of the few examples of practical use of III-V native oxides. They efficiently protect semiconductor surface after cutting, polishing and before next technological steps, e.g. epitaxial growth. Therefore, the procedure of anodic oxidation is of special importance in technology of devices based on GaSb and related compounds.

Anodic oxidation

Anodic oxidation process that takes place in liquid electrolytes is called electrolytic anodisation as opposed to gaseous anodisation, which is carried out in an ionising gas. During electrolytic anodisation the sample to be oxidised is placed on anode (hence name of the technique) and is dipped in electrolyte solution. An inert Pt electrode is used as a cathode.

Anodic oxidation process is connected with ionic transport (migration of ions on electrolyte-oxide or semiconductor-oxide interfaces) and strongly depends on electrical field intensity in the oxide. It has been shown that the thickness of the anodic oxide is a linear function of voltage applied between semiconductor and cathode [11]. However, oxide threshold current limits maximum value of oxide thickness to about 200 nm [11]. Quality and properties of anodic oxides depend on type, concentration and pH of electrolyte solution, on the method of surface preparation, intensity of electrolyte current and current efficiency of anodisation process. In anodic oxidation of GaSb 0.1N $KMnO_4$, 0.1N KOH or 30% H_2O_2 were used as electrolyte [34]. InSb has been anodic oxidised in 0.1N KOH [35–37], while InAs – in 26% H_3AsO_4, 3% $C_4H_5O_6$ and 0.1M KOH [38], [39].

Sulphuration treatment

The sulphuration technique (the surface treatment with sulphur containing solution) appears as a promising candidate for surface passivation of III-V compounds.

It has been shown that sulphur passivation significantly decreases the density of surface states in the band gap, the surface recombination velocity and, as the result, improves many device characteristics. On the other hand, it considerably decreases the oxidation rate of a semiconductor surface exposed to the atmosphere. The development of this method started in the mid -80s, but significant progress was obtained in 1990s.

A number of approaches were tried to describe the sulphur passivation. However, a comprehensive model taking account chemical and kinetic aspects of passivation is still lacking. One of the widely accepted models of semiconductor treatment in sulphide solutions [40] assumes that the chemical reaction taking place may be written in the form:

$$A^{III}B^{V} + HS^{-} + H_2O \rightarrow (A^{III})_{x'}S_{y'} + \\ + (B^{V})_{x''}S_{y''} + OH^{-} + H_2\uparrow.$$

In general, besides HS^- ions, the solution contains also S^{2-} ions and H_2S molecules. However, in the pH range from 8 to 14 the dominating ion is the HS^-. The sulphidising reaction involving S^{2-} ions and H_2S molecules proceeds in a similar way. The stoichiometric coefficients x and y can take values between 1 and 5 (for example GaS, In_2S_3, Sb_2S_3). Still, an analysis of the surface after sulphidising shows a presence of compounds like $(A^{III})_2S_3$ and/or $(B^{V})_2S_3$ [41], [42].

In the course of the sulphidizing reaction the oxidation state changes for both the semiconductor components (which are oxidised) and the hydrogen (which is reduced), so this is a kind of redox reaction and can be represented as two half-cell reactions:

$$A^{III}B^{V} \rightarrow (A^{III})^{3+} + (B^{V})^{3+} + 6e$$
$$6H^{+} + 6e \rightarrow 3H_2\uparrow.$$

According to this scheme sulphuration treatment is interpreted as the charge transfer between the semiconductor and the passivating solution. From kinetics point of view there are some factors influencing the rate of formation of passivating coat. These are the rate of charge transfer between the semiconductor and the passivating solution, the probability W_{BB} of breaking the bonds between A^{III} and B^{V} atoms and probability W_{BF} of bond formation between sulphur atoms and A^{III} and/or B^{V} atoms:

$$V = W_{BB}\, V_{ct}\, W_{BF}.$$

Every atom in the zinc blende crystal lattice is bonded to four others, each bond involving two electrons with opposite spins, whereas in the sulphide firmed at the surface each A^{III} or B^{V} atom has only three chemical bonds. This means that in the sulphidising process one of the bonds is redundant, so that for the passivating coat to be formed it is necessary that the extra electrons either enters the solution or is transferred to other energy state in the semiconductor. The first stage of passivation process is breaking of bonds between A^{III} and B^{V} atoms (Fig. 9a), next is transition of the electron localised on a dangling bond into the conduction band or to

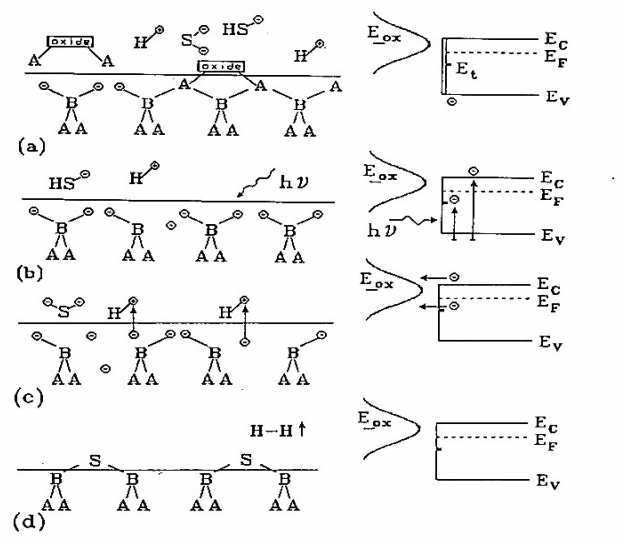

Fig. 9. Schematic diagram of the processes occurring during the formation of a sulphide passivating coating: a) breaking of bonds between A^{III} and B^{V} atoms, b) electrochemical reaction, c) escape of an electron from the semiconductor into the solution, d) formation of chemical bonds between sulphur and atoms of the semiconductor [43].

a surface state. Energy required for this, released in formation of the chemical bonds S-A^{III} and/or S-B^{V}, is provided by the photons in electrochemical reaction (Fig. 9b). Following is escape of an electron from semiconductor into the solution and formation of chemical bonds between sulphur (Fig. 9c) and atoms of the semiconductor (Fig. 9d).

2. Experimental

2.1. Samples

The following samples were used in surface treatment studies:

- (100) oriented monocrystalline 400 μm thick GaSb wafers doped with Te ($n \approx 2 \cdot 10^{17}$ cm^{-3}) and undoped p-type GaSb wafers with hole concentration $p \approx 1 \cdot 10^{18}$cm^{-3},
- 1 μm thick $In_{0.19}Ga_{0.81}As_{0.16}Sb_{0.84}$ and $Al_{0.3}Ga_{0.7}As_{0.03}Sb_{0.97}$ epilayers grown on (100) GaSb substrate,
- GaSb/ $In_xGa_{1-x}As_ySb_{1-y}$/ $Al_xGa_{1-x}As_ySb_y$ heterostructures lattice mismatched to GaSb substrate and designed for mid-infrared photodetectors (PD),
- GaSb/ $In_xGa_{1-x}As_ySb_{1-y}$/$Al_xGa_{1-x}As_ySb_{1-y}$ heterostructures lattice mismatched to GaSb substrate and designed for mid-infrared light emitting diodes (LED).

The epitaxial structures studied were grown by liquid phase epitaxy (LPE) technique. The composition of the liquid phase and the parameters of the LPE growth procedure were optimised to provide detectors operating up to the wavelength of 2.4 μm [44]. Mesa photodiodes with active area diameter of 200 μm were formed using photolithography and RIE in CCl_4/H_2 plasma. The AgTe/Ti/Au and Au/Zn/Au metallization were applied for backside n-type and front p-type ohmic contacts, respectively. The processing of device structures was completed by electrochemical passivation of mesa side-walls.

Prior to sulphur treatment the samples were cleaned in hot organic solvents and etched sequentially in $HCl + HNO_3 = 30 + 1$ at $T = 5^oC$ for $t = 20$ s and in $HCl + H_2O = 1 + 6$ at RT for 60 s.

Table 8 summarises the optimal parameters of LPE growth process for PD heterostructures which active layer compositions corresponding to λ = 2.25 μm and 2.35 μm wavelength. In Table 9 LPE process parameters for LED heterostructures with maximum emission in wavelength range 1.94 ÷ 2.35 μm are shown.

Table 8. LPE process parameters of $In_xGa_{1-x}As_ySb_{1-y}/Al_xGa_{1-x}As_ySb_{1-y}$ structures for detectors with λ = 2.25 μm and 2.35 μm.

Solid composition	Liquid atomic fractions					Growth temp. T_o [°C]	Doping	Lattice mismatch $\Delta a/a \cdot 10^{-4}$	Wavelength λ [μm]
	x^l_{Ga}	x^l_{Al}	x^l_{In}	x^l_{As}	x^l_{Sb}				
$In_{0.19}Ga_{0.81}As_{0.16}Sb_{0.84}$	0.149	–	0.595	0.0017	0.255	528	–	– (2÷5)	2.25
$Al_{0.34}Ga_{0.66}As_{0.025}Sb_{0.975}$	0.898	0.020	–	0.0002	0.080	527	Ge	+(7÷10)	
$In_{0.23}Ga_{0.77}As_{0.18}Sb_{0.82}$	0.097	–	0.400	0.0270	0.500	593	–	+(1÷5)	2.35
$Al_{0.34}Ga_{0.66}As_{0.025}Sb_{0.975}$	0.898	0.020	–	0.0002	0.080	592	Ge	– (1÷5)	

Table 9. LPE process parameters of $In_xGa_{1-x}As_ySb_{1-y}/Al_xGa_{1-x}As_ySb_{1-y}$ structures for LED with λ_p = 1.94 μm, 2.06 and 2.35 μm.

Solid composition	Liquid atomic fraction					Growth temp. T_o [°C]	Doping	Wavelength λ [μm]
	x^l_{Ga}	x^l_{Al}	x^l_{In}	x^l_{As}	x^l_{Sb}			
$In_{0.062}Ga_{0.938}As_{0.043}Sb_{0.957}$	0.457	–	0.390	0.00057	0.152	530.0	Te	
$Al_{0.21}Ga_{0.79}As_{0.02}Sb_{0.98}$	0.945	0.011	–	0.00038	0.044	529.9	Ge	1.94
p-GaSb	0.938	–	–	–	0.062	528.0	Ge	
$In_{0.084}Ga_{0.916}As_{0.086}Sb_{0.914}$	0.295	–	0.404	0.0018	0.299	593.0	Te	
$Al_{0.34}Ga_{0.66}As_{0.025}Sb_{0.758}$	0.898	0.020	–	0.0002	0.080	592.8	Ge	2.06
p-GaSb	0.889	–	–	–	0.110	592.3	Ge	
$In_{0.23}Ga_{0.77}As_{0.18}Sb_{0.82}$	0.097	–	0.400	0.0270	0.500	593.0	Te	
$Al_{0.34}Ga_{0.66}As_{0.025}Sb_{0.758}$	0.898	0.020	–	0.0002	0.080	592.6	Ge	2.31
p-GaSb	0.889	–	–	–	0.110	591.8	Ge	

2.2. Technology of surface treatment

The following techniques of semiconductor surface treatment were used in this work:

- chemo-mechanical polishing,
- anodic oxidation,
- wet etching,
- dry etching,
- deposition of passivating coatings,
- lithography.

Below some parameters of these processes are described.

Chemo-mechanical polishing

Chemo-mechanical polishing was carried out using corrosion-proof Malvern Multipol 4 polishing machine. Pocorfarm 404 as polishing material and Br_2-$C_2H_4(OH)_2$ or HF-H_2O_2-$C_4H_6O_6$ as polishing solution were used.

Anodic oxidation

Anodic oxidation was performed in $C_4H_6O_6$-$C_2H_4(OH)_2$ solution with positively biased anode; and anodic voltage in the range from 50 to 100 V.

Wet etching

In wet etching studies typical dipping technique was used. HF-, HCl-, Br_2-, or NH_4OH-based solutions as etchants and HNO_3- or H_2O_2-based solutions as oxidising agents were used. As solvents and complexing agent H_2O, CH_3OH or CH_3COOH and $C_4H_6O_6$ were applied, respectively.

Dry etching

Two techniques of dry etching were applied:

– sputter etching (dc sputtering) in a Leybold Z-400 Sputtering System;
– reactive ion etching (RIE) in a commercial Secon Mark 4 reactor.

Sputter etching was performed in Ar^+ plasma at pressure $p = 8 \cdot 10^{-3}$ mbar, frequency of plasma agitation $f = 13.5$ MHz and with positively biased substrate at the voltage $U_{DC} = 120 \div 500$ V.

RIE system with a diode configuration chamber, a 13.56 MHz power supply and 6 gas lines equipped with mass flow controllers were used. The process gas pressure was measured by a capacitance manometer. Dry etching of GaSb and related materials surface was carried out with CCl_2F_2 or CCl_4 plasma as active gas and H_2 or N_2 as gas thinner. All gases (5N BOC) were used at flow rate of $6.6 \div 23.9$ sccm and working pressure of $75 \div 162$ μbar. A source of CCl_4 was 99.8% liquid source (LAB-SCAN Analitical Sciences), while O_2 and CF_4 gases were applied for reactor cleaning.

Deposition of passivating coatings

Surface passivation was performed by dipping and electrochemical techniques.

The following sulphur sources were used:

– inorganic compounds: Na_2S, 21%$(NH_4)_2S$,
– organic compound- $(NH_2)_2CS$ (thiourea),

both in aqueous solution or in alcoholic solutions: C_3H_7OH or $C_2H_4(OH)_2$.

Electrochemical sulphuration was performed at RT and with electric current density varied in the range from $1.6 \cdot 10^{-2}$ to 35 mA/cm^2.

Lithography

Two techniques were used to define pattern on surfaces of GaSb wafers and GaSb based heterostructures:

– photolithography with the use of Carl Süss MJB 21 UV 400 alignment and exposure equipment for critical dimension (CD) above 1 μm and Carl Süss MJB UV 250/350/400 system for pattern with CD<1 μm;
– E-beam lithography with JEOL 6400 scanning microscope equipped with Raith pattern generator.

Spin coating and backing process of photo- and electron - resists were carried out using Brewer Model 100CB Hotplate/Spinner with computer control parameters: spin speed $v = 0 \div 6000$ rpm, spin time $t = 0 \div 999$ s and hot plate temperature $T = 50 \div 300^{o}$C.

2.3. Surface characterisation techniques

For complete characterisation of surface state complementary microanalytical techniques were used. They provided information on:

– topographic structure – by using optical microscopy with phase contrast (OM-NC), scanning electron microscopy (SEM), atomic force microscopy (AFM), transmission electron microscopy (TEM), spectroscopic ellipsometry (SE), and precision profilometric measurements;
– crystallographic structure – by using X-ray diffractometry (XRD) and transmission electron microscopy (TEM);
– chemical structure – by spectroscopic ellipsometry (SE) and X-ray photoelectron spectroscopy (XPS) .

For surface characterisation following experimental set-ups were used:

– optical microscopy with phase contrast – Olympus BX 51 microscope equipped with Microscope Digital Camera DP 12;
– scanning electron microscopy (SEM) – JEOL 6400 and Philips XL 30 microscopes;
– atomic force microscopy (AFM) – Digital Instruments NanoScope IIIa microscope;
– transmission electron microscopy (TEM) – JEOL JEM 200 CX microscope;
– spectroscopic ellipsometry (SE) – VASE (Variable Angle Spectroscopic Ellipsometer) ellipsometer from J. A. Woollam;
– profilometry – TENCOR α-step 200 profiler;
– X-ray diffractometry (XRD) – high-resolution Philips Material Research Diffractometer;
– X-ray photoelectron spectroscopy (XPS) – PHI 5700/660 spectrometer using monochromatised Al Kα source at energy of 1486.6 eV and the incident angle of 45^o.

The spectral line of C 1*s* ($E_B = 284.6$ eV) was used to calibrate the binding energy. The XPS database from Physical Electronics Handbook of Photoelectron Spectroscopy [45] was used as the preliminary reference for identifying the chemical states in compounds.

Ellipsometric measurements performed in the spectral range from 240 to 1100 nm at two angles of 65^o and 75^o provided information on thickness, composition and morphology of surface layers formed after surface treatment. They also allowed determining optical characteristics, first of all refractive index *n*, of the surface layer. At standard conditions the sample area of 6.0 mm^2 was examined. In the case of heterogeneous surfaces additional optical "microspot" system reducing analysed surface area to 0.12 mm^2 was used.

To extract physical information from ellipsometric data, a model dependent analysis has been performed. For every surface treatment as simple as possible nominal model was specified first and then, the complexity was added when needed to improve the data fit. The "best fit model" structures assumed for ellipsometric data analysis are shown in Fig. 10. Here, surface roughness was simulated as a 50% mixture of surface layer and air, and interface roughness ("intermix") as a 50% mixture of adjacent materials. In multilayer structures, GaSb oxide and Cauchy material (in which refractive index and extinction coefficient are represented by slowly varying function of wavelength and exponential absorption tail) either form separate layers, or two-consistent single layer described by the Brugeman Effective Medium Approximation (EMA) [46].

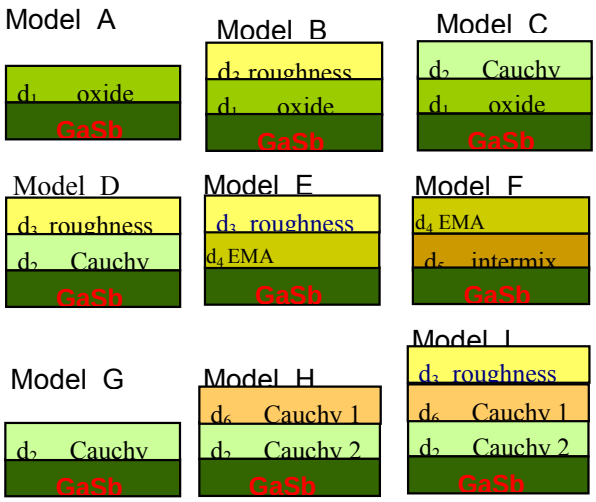

Fig. 10. The "best fit model" structures assumed for analysis of ellipsometric data.

The efficiency of passivation process was examined by measuring the current-voltage and capacitance-voltage characteristics of Schottky barrier with Au metalization deposited on GaSb passivated surface. These measurements were done with QuadTech 7600 LCR Meter and Keithley 237 High Voltage Source Measure Unit. The potentiometric and iodometric analyses have been performed to determine the total sulphide [TS] = = $[S_x^{2-}]$ + $[S^{2-}]$ and reactive sulphide [RS] = = $[S_x^{2-}]$ + $[S^{2-}]$ + $[SO_3^{2-}]$ concentrations in electro- lytes using Metrohm 721 Newt Titrino system. Basicity of solutions was measured using pH-meter pH 315i @ WTW with precision electrode SenTix @ H.

Characterisation of GaSb/InGaAsSb/AlGaAsSb device structures involved measurements of photodiode dark current and its spectral response. Spectral current responsivities have been measured using Fourier Transform Infrared (FTIR) spectro-photometer and a low noise transimpedance pre-amplifier at zero bias conditions.

3. Results and discussion

3.1. Chemo-mechanical polishing of GaSb

From various etching solutions tested, including NaOCl, HF-H_2O_2-$C_4H_6O_6$ and Br_2-ethylene glycol solutions, the last system was the only one enabling the fabrication of good GaSb surface morphology at reasonable polishing rate. However, the results obtained depended strongly on the bromine concentration (see Table 10). For high Br_2 concentration (1 + 30) the etch rate was about 9 μm/min. Then, rough and cloudy GaSb surface was observed. For lower Br_2 concentration (1 + 80) the polishing rate decreased to 3 μm/min and surface morphology improved. The use of (1 + 100) solution enabled to produce mirror-like surface at 2 μm/min polishing rate. Detailed ellipsometric and AFM measurements indicate that such a surface exhibits superficial layer thinner than 8 nm.

Table 10. Morphology of (100) GaSb surface prepared by chemo-mechanical polishing.

Solution	Compo-sition	Etch rate [μm/min]	Surface morphology
$Br_2 + C_2H_4(OH)_2$	1 + 30	9.0	Rough
$Br_2 + C_2H_4(OH)_2$	1 + 50	7.0	Smooth, dislocation etch pits
$Br_2 + C_2H_4(OH)_2$	1 + 80	3.0	Smooth, dislocation etch pits
$Br_2 + C_2H_4(OH)_2$	1 + 100	2.0	Mirror-like, without dislocation etch pits

Due to high reactivity of GaSb surface it was necessary to protect its surface against influence of atmospheric air after the polishing. This was done by covering the surface by a thin layer of anodic oxide. Anodic oxidation of GaSb surface was carried out in the $C_4H_6O_6 + C_2H_4(OH)_2$ solution. The results of measurements of ellipsometric indices Δ and Ψ presented in Figs. 11 and 12 indicate that parameters of oxide layers formed by this method agree with literature data [47]. Using ellipsometric measurements the dependence of oxide layer thickness on anodisation parameters has also been determined (Table 11).

For final optimalisation of GaSb surface polishing the following three procedures were compared:

A) mechanical polishing and etching in $Br_2 + C_2H_4(OH)_2$ = 1+100;
B) chemo-mechanical polishing in $Br_2 + C_2H_4(OH)_2$ = =1 + 100;
C) chemo-mechanical polishing in $Br_2 + C_2H_4(OH)_2$ = =1 + 100 followed by
– anodic oxidation in $C_4H_6O_6 + C_2H_4(OH)_2$ followed by
– removal of anodic oxide in HCl +H_2O = (1 + 6).

The results of ellipsometric measurements Δ(λ) illustrated in Fig. 13 and data on superficial layer thickness collected in Table 12 indicate that the procedure C gives the best results, i.e. the thinnest superficial layer (d = 1.45 nm) with surface roughness of 0.4 nm. The AFM micrographs showed in Fig. 14 confirm that this process leads to the smallest roughness of the surface (*RMS* = 0.3 nm).

Table 11. The dependence of the anodic oxide thickness on oxidation voltage.

Anodic oxidation	Spectroscopic ellipsometry (for λ = 630 nm)				
Solution	Voltage [V]	Model	Thickness [nm]	Refractive index n	Extinction coefficient k
$C_4H_6O_6$+$C_2H_4(OH)_2$ pH = 6.1	50.0	B	d_3 = 3.05 ± 0.2 d_1 = 139.70 ±0.2	1.97± 0.002	0.00
	75.0	B	d_3 = 3.22 ± 0.2 d_1 = 209.18 ±0.2	1.97± 0.002	0.00
	100.0	B	d_3 = 4.35 ± 0.2 d_1 = 281.53 ±0.3	1.97± 0.002	0.00
*Models, d_1 and d_3 parameters are defined in Fig. 10.					

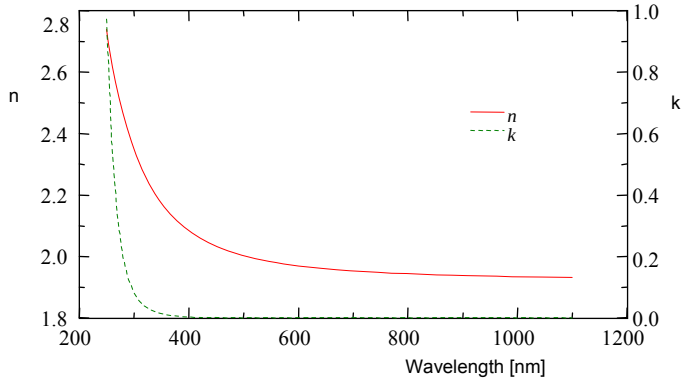

Fig. 11. Spectroscopic ellipsometric characteristics n and k of anodic oxide on (100) GaSb surface.

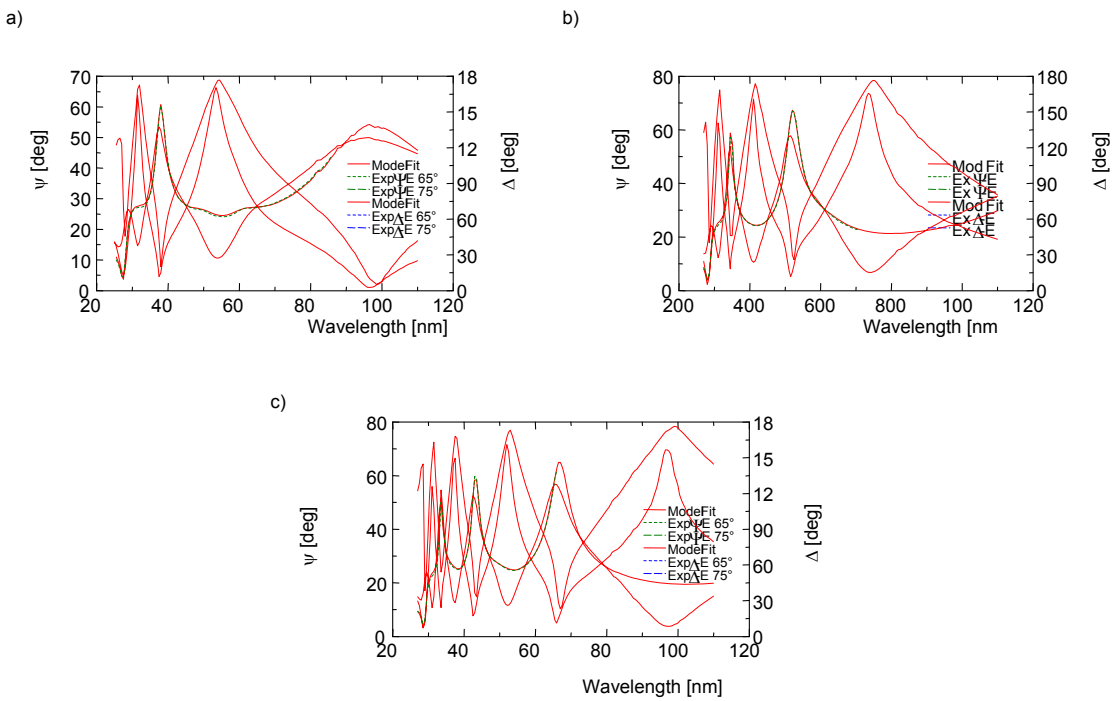

Fig. 12. Spectroscopic ellipsometric characteristics Δ and Ψ of anodic oxide obtained on (100) GaSb surface at: a) U_a = 50 V, b) U_a = 5 V, c) U_a = 100 V.

Table 12. Characteristics of polished (100) GaSb substrates.

Surface treatment	Spectroscopic ellipsometry (for λ = 630 nm)			
	Model	Thickness of superficial layer [nm]	Refractive index n	Extinction coefficient k
Two step treatment: – mechanical polishing – etching in $Br_2 + C_2H_4(OH)_2 = (1+100)$, $t = 3$min	B	$d_3 = 8.78 \pm 0.4$ $d_1 = 0.47 \pm 0.3$	1.94 ± 0.1	0
One step treatment: chemo-mechanical polishing in $Br_2 + C_2H_4(OH)_2 = (1 + 100)$	D	$d_3 = 3.00 \pm 0.1$ $d_2 = 5.16 \pm 0.4$	1.55 ± 0.1	0
Sequence: – chemo-mechanical polishing in $Br_2 + C_2H_4(OH)_2 =$ $= (1 + 100)$ – anodic oxidation in $C_4H_6O_6 + C_2H_4(OH)_2$@pH = 6.1, $U = 50$V, d_{ox}=140 nm – etching in $HCl + H_2O = (1 + 6)$, $t = 1$ min.	B	$d_3 = 0.40 \pm 0.2$ $d_1 = 1.05 \pm 0.1$	1.94 ± 0.1	0

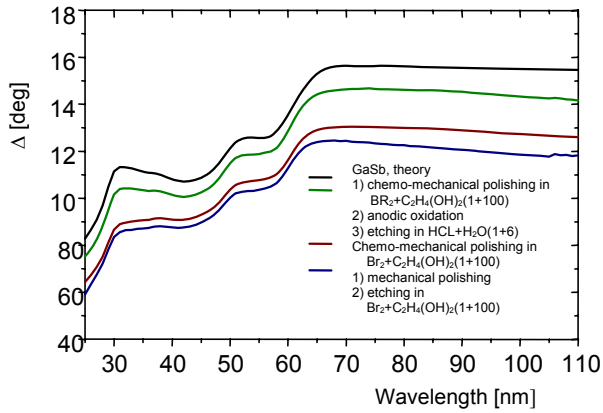

Fig. 13. The influence of (100) GaSb surface treatment on spectroscopic ellipsometric characteristics Δ(λ). Theoretical curve of GaSb surface according to J. A. Woollam Co. Inc. WVASE 32 program v 3.386, tabulated at UNL (Lincoln University, Nebraska, USA).

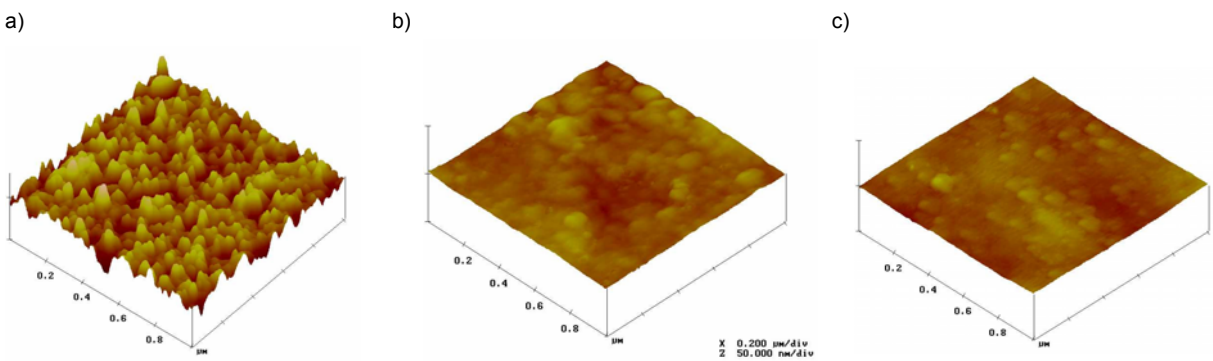

Fig. 14. AFM micrographs of (100) GaSb surface after: a) two-step treatment: •mechanical polishing, •etching in $1Br_2 + 100\ C_2H_4(OH)_2$, $t = 3$ min.; b) chemo-mechanical polishing in $1\ Br_2 + 100\ C_2H_4(OH)_2$; c) sequence surface treatment •chemo-mechanical polishing in $1Br_2 + 100\ C_2H_4(OH)_2$, •anodic oxidation in $C_4H_6O_6 + C_2H_4(OH)_2$@pH = 6.1, $U = 50$ V, $d_{ox} =$ = 140 nm, •etching in $1\ HCl + 6\ H_2O$, $t = 1$ min.

3.2. Wet etching of GaSb

Table 13 shows a list of chemical solutions examined in the present work. For selected solutions dependence of etched depth on etching time and typical step profiles after etching are shown in Figs. 15–20. The effect of surface treatment on the thickness of superficial layers, their optical constants n and k (at the wavelength $\lambda = 630$ nm) as well as values of surface roughness are given in Table 14. The character of ellipsometric dependencies Δ(λ) and $\varepsilon_2(E)$ (Figs. 21 and 22) agrees with available literature data [48], [49].

Note that HF, HCl and NH_4OH-based solutions etch (100) GaSb very slowly (≤ 50 nm/min). Usually, slow etching results in thinner native oxides. In this respect, the HCl-based solutions seem to be more favourable than the HF-based ones. In particular, surface treatment in $1HCl + 6H_2O$ system reduces the thickness of the oxide to about 0.9 nm leaving the surface roughness of $RMS = 1.65$ nm, while after

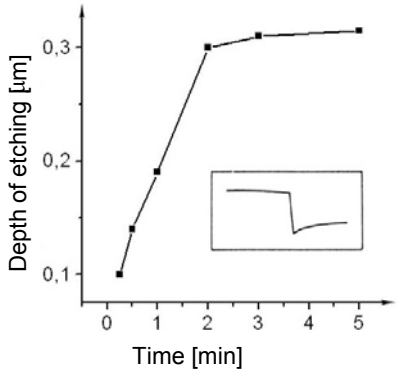

Fig. 15. The dependence of etch depth on time and step profile for 100 GaSb surface etched in HCl + HNO_3 (30 + 1) @ $T = 5^oC$.

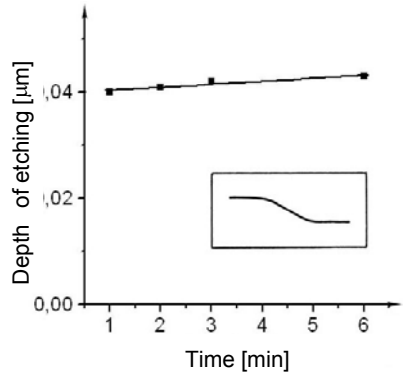

Fig. 16. The dependence of etch depth on time and step profile for 100 GaSb surface etched in 37% HCl.

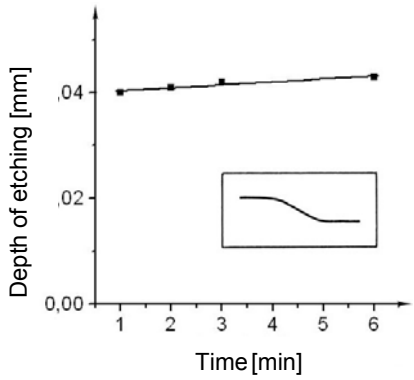

Fig. 17. The dependence of etch depth on time and step profile for 100 GaSb surface etched in 0.02M Br_2 + 0.02M HNO_3 + + (0.80M HCl + CH_3COOH).

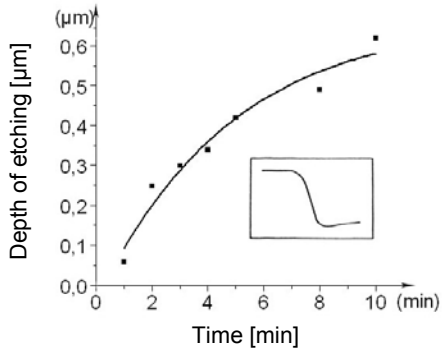

Fig. 18. The dependence of etch depth on time and step profile for 100 GaSb surface etched in NH_4OH + H_2O = (1 + 10).

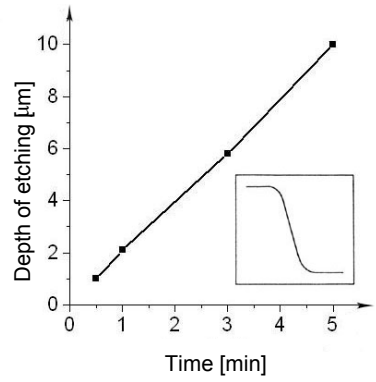

Fig. 19. The dependence of etch depth on time and step profile for 100 GaSb surface etched in 1M $C_4H_6O_6$ + 29M HF + 10M H_2O = =(40 + 2 + 0.5).

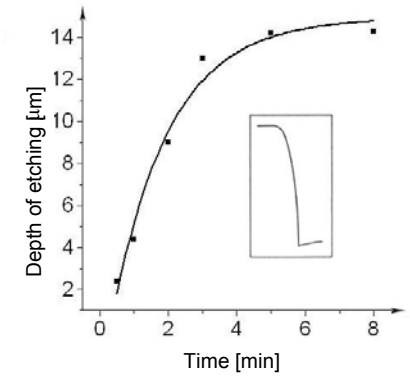

Fig. 20. The dependence of etch depth on time and step profile for 100 GaSb surface etched in HCl + H_2O_2 + H_2O = = (60+1+1).

etching in 1HF + $6H_2O$ the respective values of oxide thickness and *RMS* are about 1.2 nm and 2.8 nm. Thus, these two procedures seem to be suitable for removing of residual oxides from GaSb surface. The solutions containing strong oxidisers exhibit higher etch rate. Then however, quality of surface is worse.

For shallow etching of GaSb, two-step treatment is suitable. First, surface damage has to be removed by etching with a few hundred nm/s etching rate. Next, thick oxide formed in low-rate etchants is removed. In this category, surface treatment in 30HCl + $1HNO_3$ followed by 1HCl + $6H_2O$ etch produces GaSb surface with residual oxide layer of $d \approx 1.6$ nm thick and roughness $RMS \approx 0.6$ nm (Fig. 23). In the category of low-rate etchants, the 60HCl + $1H_2O$ + $1H_2O_2$ solution was the one giving the best results: mirror-like surface with surface roughness $RMS \approx 7$ nm and thickness of the superficial layer $d \approx 3$ nm. Thus the latter system is useful for GaSb patterning unless poor anisotropy, inherent to wet etching, is not critical. Figure 24 shows SEM micrograph and step profile of GaSb stripe structure produced by this procedure.

For chemical thinning of GaSb substrate high etching rate is required. Our studies show that optimal results are obtained for the 1HF + $14H_2O_2$ + + $20H_2O$ solution that gives GaSb etching rate of 10 µm/min.

XPS technique has been applied to analyse composition of oxide layers on wet etched (100)

Table 13. Etching characteristics of (100) GaSb.

Etching solution	Composition	Etch rate [nm/min]	Surface morphology
$HCl + H_2O$	1+6	3.0	Mirror-like
$HCl + CH_3OH$	1+3	3.0	Mirror-like
HCl	37%	40.0	Smooth
$HF + H_2$	1+6	6.0	Smooth
$HF + NH_4F + H_2O$	2+7+1	8.0	Smooth
$NH_4OH + H_2O$	1+10	50.0	Smooth
$HCl + HNO_3$@T = 5°C	30+1	200.0	Mirror-like
0.02M Br_2 + 0.02M HNO_3 + (0.80M HCl + CH_3COOH)	1+1+(1+1)	100.0	Smooth
0.02M Br_2 + 0.02M HNO_3 + (0.08M HCl + CH_3COOH)	1+1+(1+1)	500.0	Smooth
$HCl + H_2O_2 + H_2O$	60+1+1	$4.4 \cdot 10^3$	Mirror-like
$HF + H_2O_2 + H_2O$	1+4+15	$3.0 \cdot 10^3$	Smooth
$HCl + HNO_3 + CH_3COOH$	2+18+40	$6.9 \cdot 10^3$	Smooth
$HF + H_2O_2 + C_4H_6O_6$	1+14+20	$1.0 \cdot 10^4$	Smooth
1M $C_4H_6O_6$ + 29M HF + 10M H_2O	40+2+0.5	$2.2 \cdot 10^3$	Smooth

Table 14. The influence of chemical etching on optical properties of (100) GaSb.

Surface treatment	Spectroscopic ellipsometry (for λ=630nm)			
	Model	Thickness of superficial layer [nm]	Refractive index *n*	Extinction coefficient *k*
$HCl + H_2O$=(1 + 6), *t* = 3 min.	B	$d_3 = 1.65 \pm 0.1$ $d_1 = 0.91 \pm 0.1$	 1.94 ± 0.10	 0
$HCl + CH_3OH$=(1 + 3), *t* = 3 x 1min.	B	$d_3 = 0.09 \pm 0.2$ $d_1 = 1.29 \pm 0.1$	 1.94 ± 0.10	 0
37% HCl, *t* = 1 min.	B	$d_3 = 1.70 \pm 0.1$ $d_1 = 0.80 \pm 0.1$	 1.94 ± 0.10	 0
$HF + H_2O$=(1+6), *t = 1* min	C	$d_2 = 2.77 \pm 0.1$ $d_1 = 1.23 \pm 0.1$	1.6 ± 0.05 1.94 ± 0.10	0 0
$HF + NH_4F + H_2O$=(2+7+1), *t* = 1 min.	C	$d_2 = 2.00 \pm 0.1$ $d_1 = 1.22 \pm 0.2$	1.58 ± 0.01 1.94 ± 0.10	0 0
$NH_4OH + H_2O$=(1 + 10), *t* = 1 min.	C	$d_2 = 2.27 \pm 0.1$ $d_1 = 1.62 \pm 0.2$	1.78 ± 0.05 1.94 ± 0.10	 0
$HCl + H_2O_2 + H_2O_2$=(60 + 1+ 1), *t* = 1 min.	D	$d_3 = 7.05 \pm 0.44$ $d_2 = 3.01 \pm 0.30$	 1.88 ± 0.30	 0
•$HCl + HNO_3$=(30 + 1)@*T* = 5°C, *t* = 0.33 min. •$HCl + H_2O$=(1 + 6), *t* = 1 min.	C	$d_2 = 0.26 \pm 0.21$ $d_1 = 1.34 \pm 0.21$	2.30 ± 0.03 1.94 ± 0.10	0 0

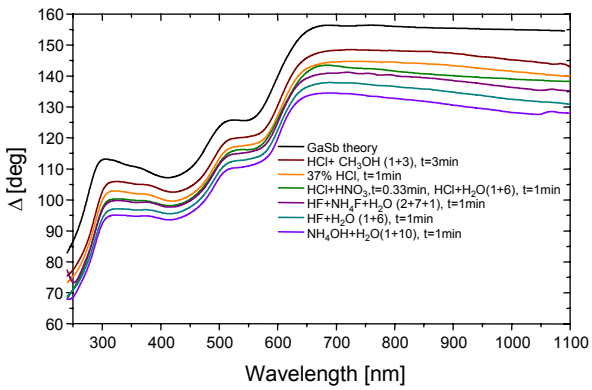

Fig. 21. Influence of chemical etching on spectral characteristics Δ(λ) of (100) surface. Theoretical curve of GaSb surface according to J. A. Woollam Co. Inc. WVASE 32 program v 3.386, tabulated at UNL (Lincoln University, Nebraska, USA).

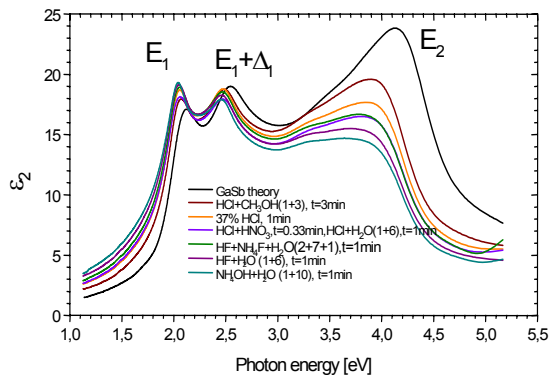

Fig. 22. Imaginary part ε_2 (*E*) of the dielectric function of (100) GaSb surface after chemical etching. Theoretical curve of GaSb surface according to J. A. Woollam Co. Inc. WVASE 32 program v 3.386, tabulated at UNL (Lincoln University, Nebraska, USA).

GaSb surface. The results obtained indicate that as the result of chemical reaction not only gallium and antimony oxides but also elemental Sb is left on the surface. Figure 25 shows XPS survey spectrum of GaSb surface etched in $1HCl + 1H_2O$. Then, Fig. 26 and Fig. 27 show fragments of this spectrum (Sb 3*d* and Ga 2*p* core levels, respectively). The XPS spectra of Sb 3*d* doublets indicates the presence of Sb_2O_3

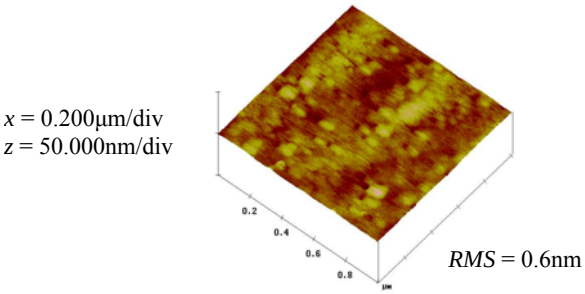

Fig. 23. AFM micrograph of (100) GaSb surface after chemical treatment: •HCl + HNO_3 = (30 + 1) @ $T = 5^oC$, $t = 0.33$ min, •HCl + H_2O = (1 + 6), $t = 1$ min.

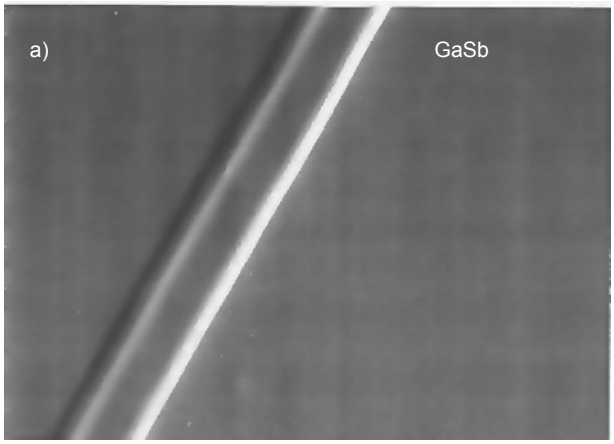

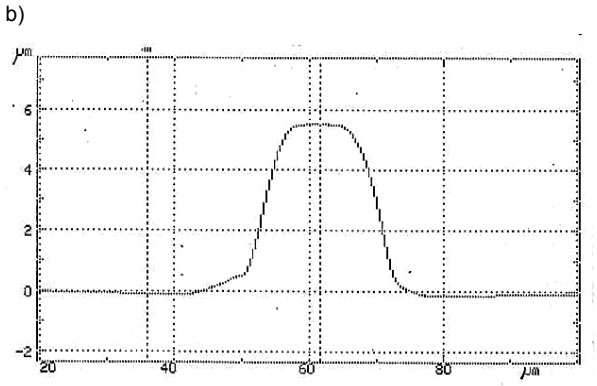

Fig. 24. SEM micrograph of GaSb surface etched in HCl + H_2O_2 + H_2O (60+1+1) (a), and the α-step profile of the etched feature (b). The stripe is 10 µm wide and 5.8 µm high.

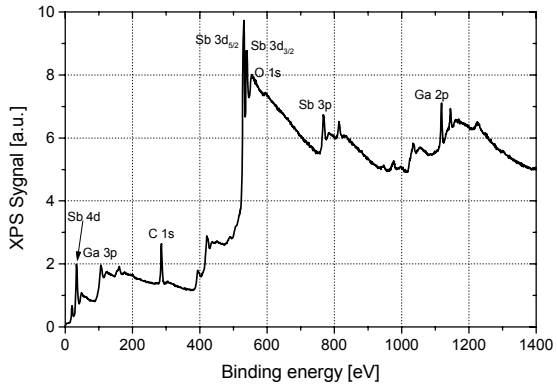

Fig. 25. The XPS survey spectrum of GaSb surface etched in 1HCl + 6H_2O, $t = 3$ min.

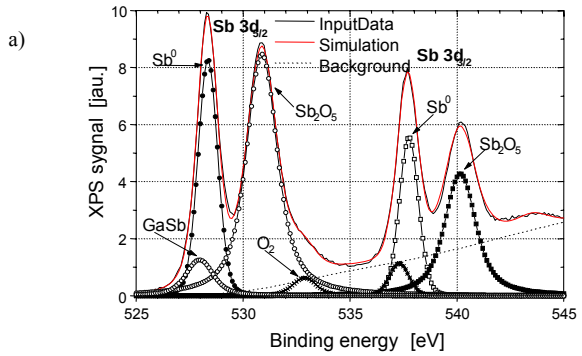

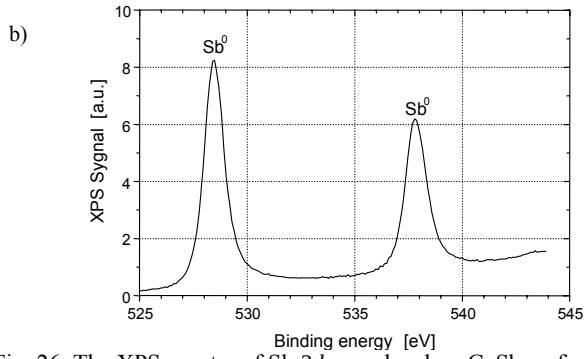

Fig. 26. The XPS spectra of Sb *3d*, core level on GaSb surface (a) etched in 1 HCl + 6 H_2O, $t = 3$ min.; b) Sb surface after sputter etching in Ar^+ at $U_{DC} = 4$ keV, $t = 1$ min.

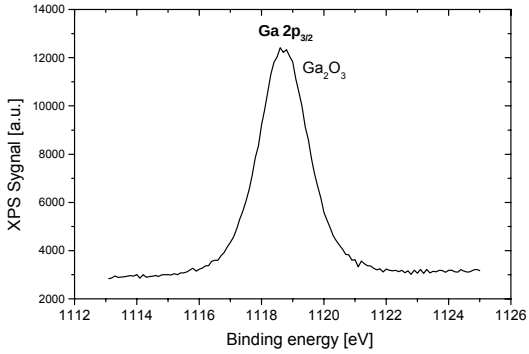

Fig. 27. The XPS spectrum of Ga *2p*, core level on GaSb surface etched in 1HCl + 6H_2O, $t = 3$ min.

Sb $3d_{3/2}$) and elemental Sb (E_B = 528.3 eV for Sb $3d_{5/2}$ and $E_B = 537.7$ eV for Sb $3d_{3/2}$) on the surface. Since binding energies for Sb and GaSb are similar position of the Sb 3*d* doublet in GaSb was compared with position of Sb line for pure Sb. In this way we confirmed that lines with binding energy $E_B = 528.3$ eV and $E_B = 537.7$ eV are descended from metallic Sb.

As anticipated, chemical solutions tested exhibit significant etching selectivity. Figure 28 presents etched depth in GaSb, $In_{0.22}Ga_{0.78}As_{0.18}Sb_{0.82}$ and $Al_{0.34}Ga_{0.66}As_{0.025}Sb_{0.975}$ versus etching time in 60HCl + 1H_2O_2 solution. These results show that wet etching process is not suitable for etching of mesa structures in GaSb-based heterostructures. Thus, alternative processes of dry etching must be considered for that purpose.

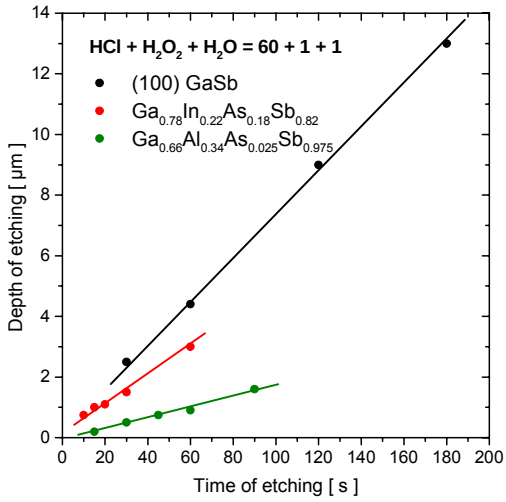

Fig. 28. Dependence of etch depth on time for GaSb, $In_{0.22}Ga_{0.78}As_{0.18}Sb_{0.82}$ and $Al_{0.34}Ga_{0.66}As_{0.025}Sb_{0.975}$ surfaces. Etching in $60HCl + 1H_2O_2 + 1H_2O$ solution.

3.3. Dry etching of GaSb

3.3.1. Sputter etching

Sputter etching in Ar^+ plasma would be an attractive method of *in-situ* surface preparation prior to metal deposition if ion-induced damage of semiconductor surface could be minimised. The thickness of defected layer can be reduced by optimisation of DC voltage and sputter etching time. Influence of parameters of sputter etching on properties of (100) GaSb surface are illustrated by data shown in Table 15 and in Figs. 29–30. The

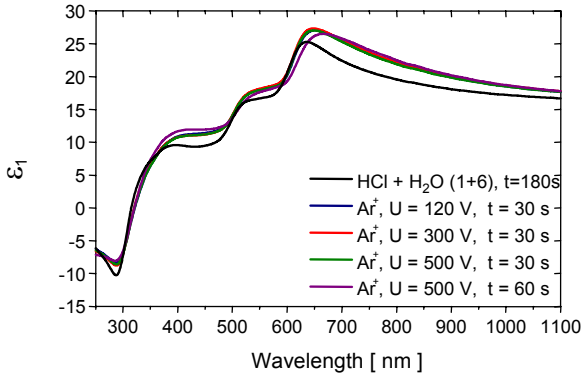

Fig. 29. The spectral characteristics $\varepsilon_1(\lambda)$ and $\varepsilon_2(\lambda)$ of (100) GaSb after Ar^+ sputter and wet etching in $6HCl + 1H_2O$.

characteristics of native oxide obtained on (100) GaSb surface as a result of wet etching in $6HCl + 1H_2O$ are also included for comparison.

The results indicate presence of a damage layer with refractive index $n \approx 5.2 \div 5.3$ and extinction index $k \approx 1.5$. Thus, the surface is free from native oxide ($n_{ox} = 1.94$), though the GaSb surface is damaged ($n_{GaSb} = 5.052$). The characteristic of imaginary part $\varepsilon_2(E)$ of dielectric function is the most sensitive to degree of surface damage. Results shown

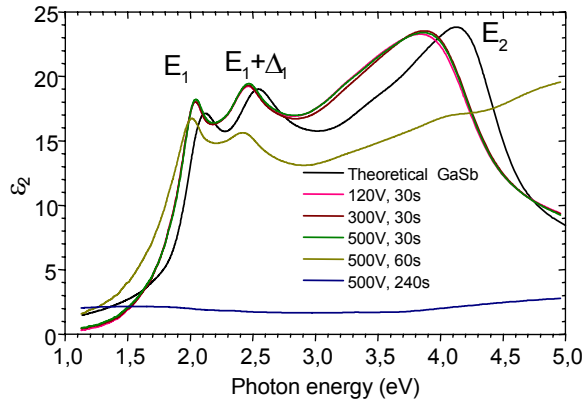

Fig. 30. The spectral characteristics $\varepsilon_2(E)$ of GaSb surface after Ar^+ sputter etching andwet etching in $6HCl + 1H_2O$. Theoretical curve of GaSb surface according to J. A. Woollam Co. Inc WVASE 32 program v 3.386, tabulated at UNL (Lincoln University, Nebraska, USA).

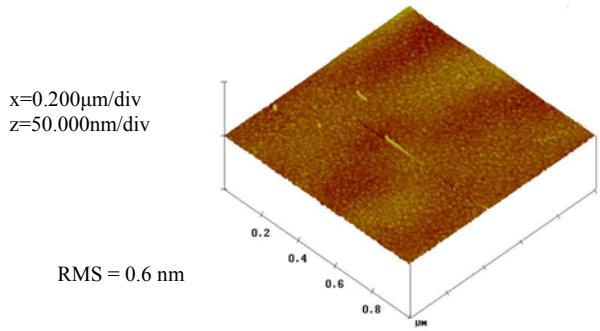

Fig. 31. AFM micrograph of (100) GaSb surface after sputter etching in Ar^+ plasma ($U_{DC} = 300$ V, $t = 30$ s).

in Fig. 30 confirm that thickness and degree of surface damage increase with increasing of DC voltage and sputter etching time. Thus, the best results were obtained by reducing DC voltage to $U_{DC} = 300$ V, that corresponds to etching rate of 6 nm/min, and limiting the etching time to $t = 30$ s. AFM micrograph of GaSb surface prepared in that way is shown in Fig. 31.

3.3.2.Reactive ion etching (RIE)

RIE experiments were performed with aim to develop a procedure of anisotropic etching required in the processing of optoelectronic device structures. The plasma chemistry has been identified as the key factor controlling etching characteristics of GaSb and relative semiconductors. Feed gas composition had a decisive influence on the etch rate, the microscopic etch uniformity and the suitability of RIE for the anisotropic etching of GaSb/InGaAsSb/AlGaAsSb heterostructures.

Figure 32 shows the GaSb etch depth in CCl_2F_2/N_2 and CCl_4/N_2 plasmas as a function of active chemical etching species CCl_2F_2 or CCl_4 concentration. The following Figs. 33a, 34a and 35a show similar set of data for CCl_2F_2/H_2, CCl_4/H_2 and BCl_3/Ar plasmas. Etching in CCl_4-based plasma has

been found much faster than RIE in plasmas involving CCl_2F_2. Most presumably this is due to the higher concentration of reactive chlorine. For similar process parameters the lowest etch rates were observed when RIE was performed in CCl_2F_2/N_2 plasmas, whereas etching in CCl_4/N_2 resulted in the highest etch rates. Although an increase of surface roughness was observed after some high-rate RIE processes, it was relatively easy to optimise process parameters to obtain GaSb surfaces with the roughness below 5 ÷ 10 nm still keeping relatively high etching rate in the range from 1.5 to 2 μm/min. Replacement of nitrogen by hydrogen in plasma containing CCl_2F_2 led to increase of etch rate, as illustrated in Figs. 33a and 34a, with simultaneous deterioration of etched surface morphology. On the other hand, addition of H_2 instead of N_2 to CCl_4 causes a decrease of etch rate by a factor of 8 ÷ 10 (Fig. 33b, 35a) preserving good morphology of the etched surface. GaSb etched in H_2-diluted plasmas show little change in etch rate until a concentration of about 45% by volume of active gas is reached. Then the etch rate increases sharply. Presumably, this rapid increase starts only when the concentration of active chlorine species available for the reaction at the semiconductor surface achieves a sufficiently high level.

Tabl. 15. The influence of Ar^+ sputter etching on (100) GaSb surface state.

Surface treatment		Spectroscopic ellipsometry (for λ = 630nm)			
Ion etching		Model	Thickness of superficial layer [nm]	Refractive index *n*	Extinction coefficient *k*
U [V]	*t* [s]				
120	30	G	$d_2 = 3.69 \pm 0.84$	5.31	1.45
300	30	G	$d_2 = 3.73 \pm 0.86$	5.18	1.43
500	30	G	$d_2 = 3.74 \pm 0.73$	5.32	1.43
500	60	G	$d_2 = 3.84 \pm 0.23$	5.29	1.57
Wet etching in HCl +H_2O = (1 + 6); *t* = 3 min.		B	$d_3 = 1.65 \pm 0.10$ $d_1 = 0.91 \pm 0.10$	1.94	0

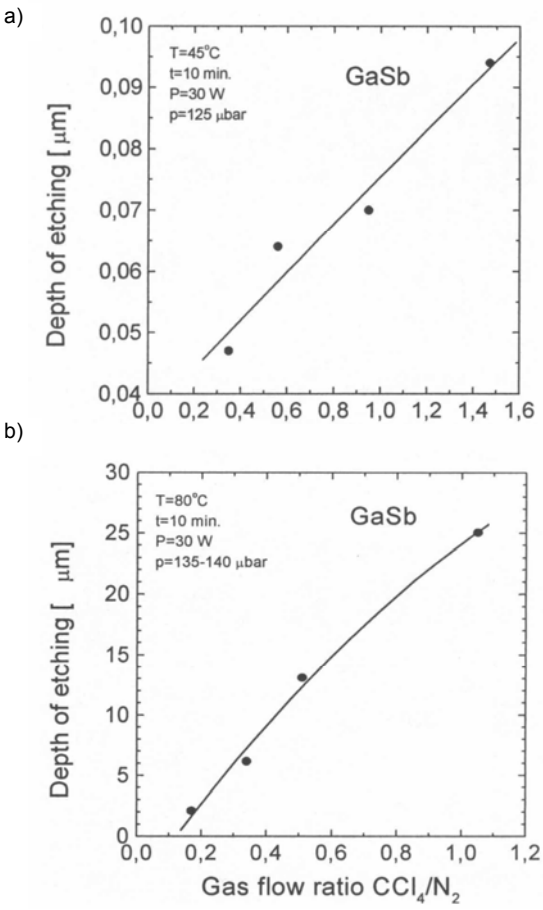

Fig. 32. Etching in CCl_2F_2/N_2 (a) and CCl_4/N_2 (b)discharges as a function of feed gas composition.

Plots of the etch depth of GaSb as a function of rf power (Figs. 33b, 34b and 35b) and processing power (Figs. 33c, 34c and 35c) show that with increasing values of these parameters the etch rate monotonically increases. Most probably, this is the result of the enhancement of ion bombardment energy and an increasing generation of radicals. The most important finding, with regard to quaternary materials, is very large resistance of InGaAsSb and AlGaAsSb against etching in CCl_2F_2-based plasma and low etch rate of InGaAsSb in CCl_4/N_2 plasma. In contrast, etching rates of AlGaAsSb and InGaAsSb epilayers in CCl_4/H_2 or BCl_3/Ar plasmas are comparable and similar to the etch rate of GaSb (Figs. 35a, 35d and 36b). Careful analysis of the results obtained indicates that by optimising RIE conditions an anisotropic etching of GaSb/InGaAsSb/AlGaAsSb device heterostructures is feasible.

In summary, it is important to point out that application of CCl_4 plasma gives higher etching rate, while advantage of using BCl_3-based plasma is better morphology of etched surface.

3.4. Passivation of GaSb surfaces

3.4.1. Chemical sulphuration by dipping technique

All the structures used in our studies on surface passivation were exposed to surface pre-treatment consisting of: a) anodic oxidation in $C_4H_6O_6 + C_2H_4(OH)_2$ system at $U = 50$ V, b) removal of anodic oxide in HCl + H_2O = (1 + 6) for 1 min. directly prior to sulphuration treatment. After sulphuration the samples were rinsed in izopropanol and finally blown dry with nitrogen.

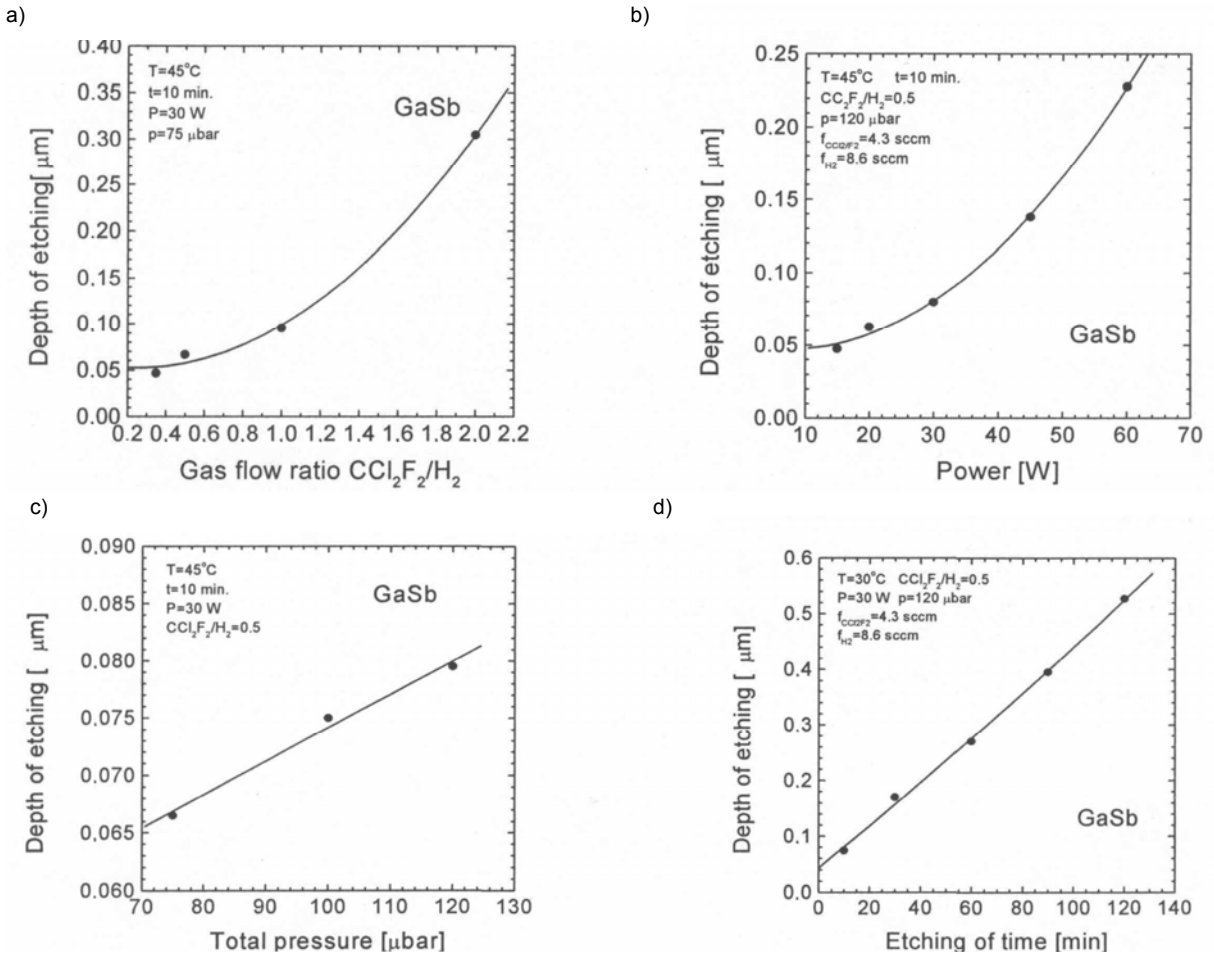

Fig. 33. Etching of (100) GaSb in CCl_2F_2/N_2 discharges. Influence of: a) feed gas composition, b) rf power, c) working pressure, d) etching time.

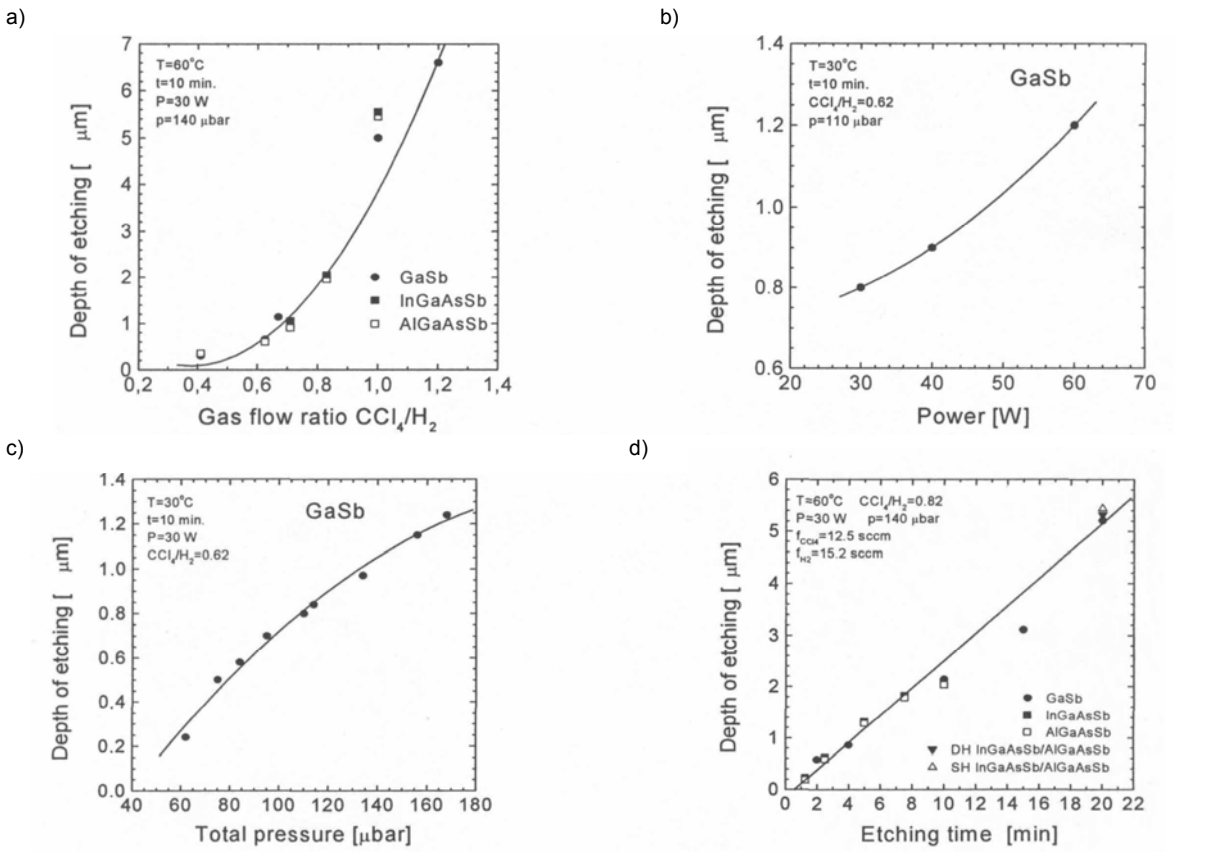

Fig. 34. Etching of (100) GaSb, (100) InGaAsSb and (100) AlGaAsSb in CCl_4/H_2 discharges. Influence of: a) feed gas composition, b) rf power, c) working pressure, d) etching time.

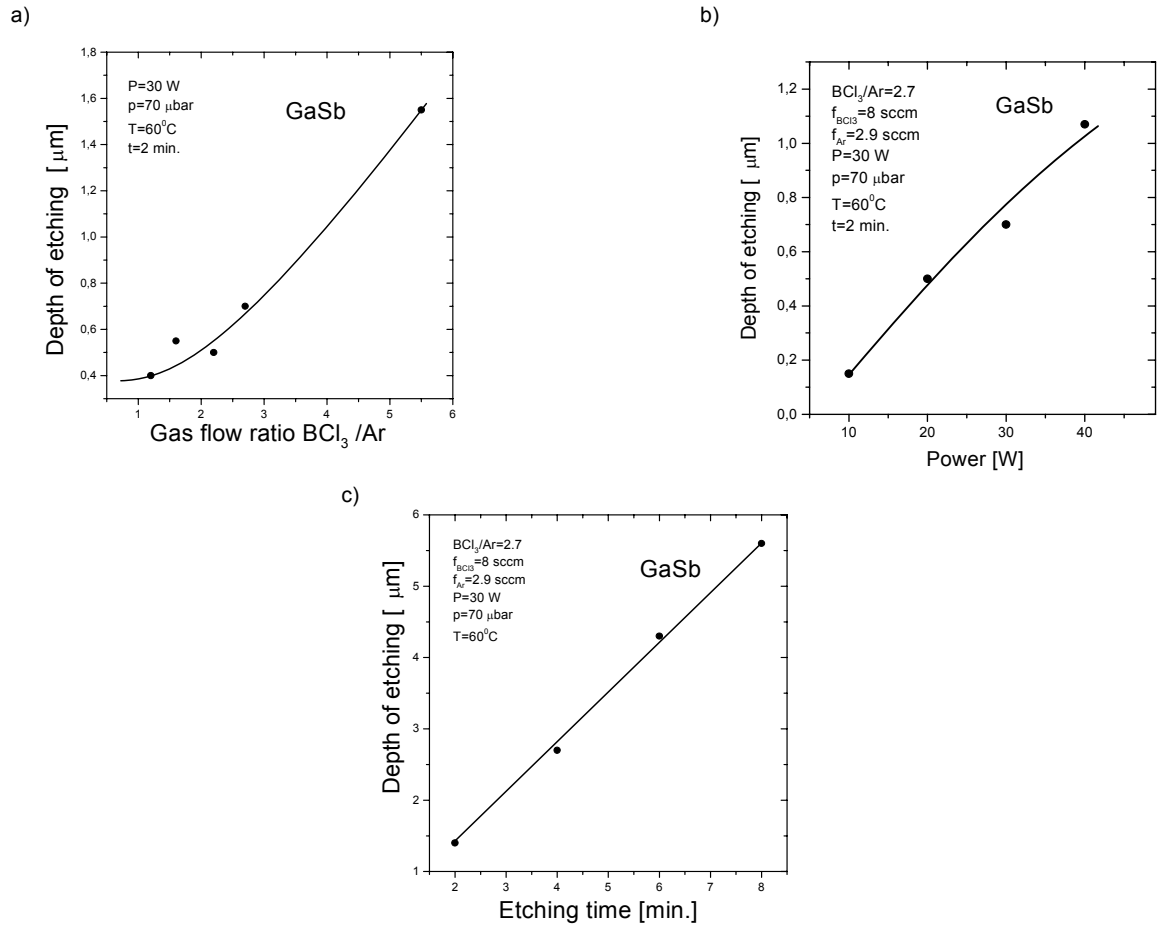

Fig. 35. Etching of (100) GaSb in BCl_3/Ar plasma. Influence of: a) feed gas composition, b) rf power, c) etching time.

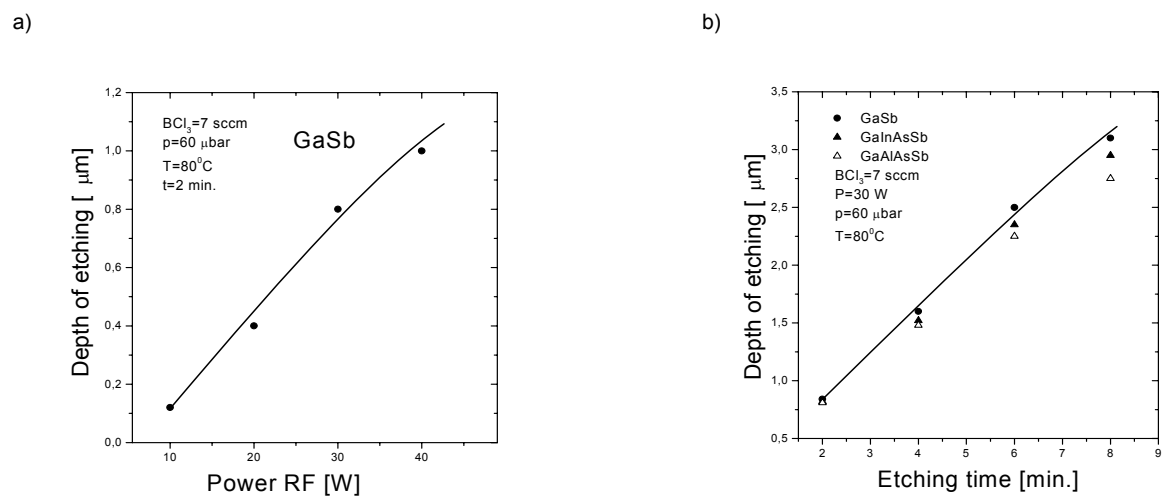

Fig. 36. Etching of (100) GaSb, (100) InGaAsSb and (100) AlGaAsSb in BCl_3 plasma. Influence of: a) rf power, b) etching time.

Before studying passivation of GaSb-based semiconductors we decided to check if they are etched by sulphur-containing solutions. This is of prime importance if the passivation procedure is to be applied for GaSb-based devices containing thin epitaxial layers. Our results show that all solutions used etch III-V semiconductors studied. Figure 37 shows the influence of chemical composition and temperature of sulphur containing solution on etching rate of GaSb surface. As it is seen 21% $(NH_4)_2S$-H_2O system gives higher etch rate than 16% Na_2S-H_2O system. In addition, increase of solution temperature increases surface etching rate. The influence of III-V compound composition and of $(NH_4)_2S$-H_2O solution concentration on surface etching rate is shown in Fig. 38. As anticipated, the etching of semiconductors with different chemical compositions proceeds with different rates. Note in this context that

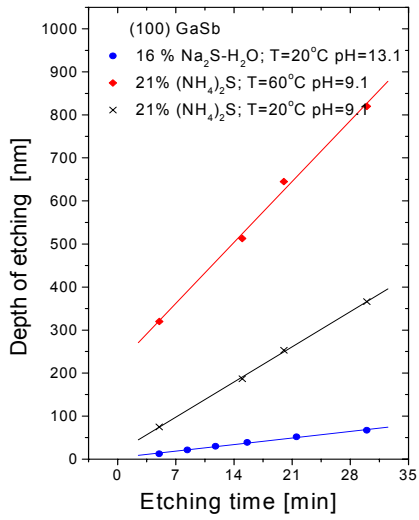

Fig. 37. The influence of sulphur source and temperature on etching rate of (100) GaSb surface.

a)

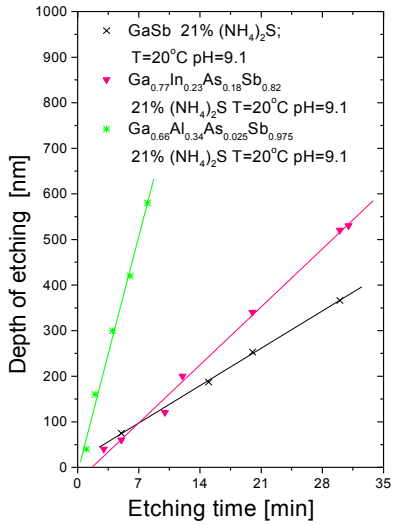

b)

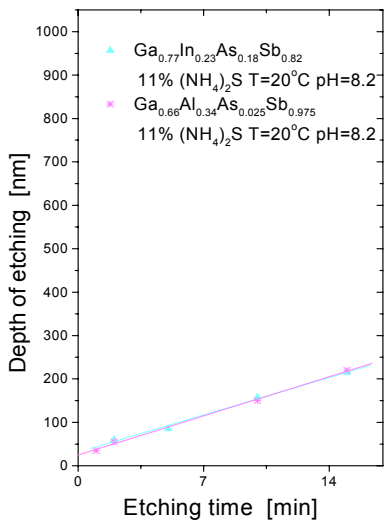

Fig. 38. The influence of III-V compound composition and of $(NH_4)_2S$-H_2O system concentration on etching rate of GaSb-based compound surface.

decrease of $(NH_4)_2S$ concentration to 11% (Fig. 38b) allows for equal etching rates of $In_{0.23}Ga_{0.77}As_{0.18}Sb_{0.82}$ and $Al_{0.34}Ga_{0.66}As_{0.025}Sb_{0.975}$.

Variable Angle Spectroscopic Ellipsometry (VASE) and X-ray Photoelectron Spectroscopy (XPS) were applied to characterise the GaSb surface after passivation. The results of ellipsometric measurements, namely thickness of surface layer, its refractive index and extinction coefficient, are summarised in Table 16.

The XPS measurements provided information on chemical composition of passivated surfaces.

Since XPS standard data for surface including gallium and antimony sulphides are not available, the XPS measurements of Ga_2S_3, Sb_2S_3 and Sb_2S_5 standard samples were carried out. The results are shown in Figs. 39, 40, and 41 where the survey spectra and the spectra of Ga $2p_{3/2}$, Sb $3d$ and S $2s$ signals are displayed. These enabled the evaluation of binding energies of Ga_2S_3, Sb_2S_3, and Sb_2S_5, which are presented in Table 17.

It should be noted that for Ga_2S_3, besides the main single spectral lines of Ga $2p_{3/2}$ and S $2s$, photoelectron and Auger lines from oxygen and carbon are clearly visible. The Sb_2S_3, the spectrum of spin-orbit doublet of Sb $3d_{5/2}$ shows distinct low-binding-energy features. This suggests possible surface instability of this material. Both Sb_2S_3 and Sb_2S_5 are characterised by very similar binding energies.

All the results presented above indicate that as the result of sulphur passivation the (100) GaSb surface is covered by a thin sulphur containing layer. Its structure and properties (layer thickness, chemical composition, optical properties and surface morphology) depend on treatment time and on composition of the solution.

The spectral ellipsometric characteristics $\Delta(\lambda)$ show (Fig. 42) that the (100) GaSb surface undergoes a significant modification after relatively short time (45 s) of passivation. They show also, that besides a type of sulphur source – Na_2S or $(NH_4)_2S$, also a choice of solvent determines efficiency of surface modification. This is even more clearly visible in Fig. 43 that shows dependence of modified layer thickness on treatment time for different sulphur sources and different solvents used for (100) GaSb surface passivation. As it is seen, replacement of H_2O solvent in Na_2S based solution by izopropanol increases significantly modified surface layer thickness. Then, it becomes even larger than that obtained with the use of 21% $(NH_4)_2S$-H_2O system. Simultaneously, roughness of the surface treated by the Na_2S solution is smaller if izopropanol instead of water is used as the solvent (see Fig. 44).

Table 16. Characteristics of (100) GaSb surface after chemical passivation.

Surface treatment						Spectroscopic ellipsometry for λ = 630 nm			
Solution	[RS]	[TS]	pH	$[NH_4^+]$	Time [min.]	Model	Layer thickness [nm]	Refract. index n	Extinct. coeff. k
16% Na_2S-H_2O	0.4	0.34	–	13.1	0.25	C	$d_2 = 0.66 \pm 0.10$ $d_1 = 1.17 \pm 0.10$	1.94	0.00
					0.50	C	$d_2 = 1.10 \pm 0.10$ $d_1 = 1.40 \pm 0.10$	1.95	0.00
					0.75	C	$d_2 = 1.35 \pm 0.10$ $d_1 = 1.45 \pm 0.10$	1.95	0.00
					1.00	C	$d_2 = 1.97 \pm 0.10$ $d_1 = 1.57 \pm 0.10$	1.79	0.16
					3.00	C	$d_2 = 2.48 \pm 0.15$ $d_1 = 1.95 \pm 0.26$	1.95	0.18
					10.00	C	$d_2 = 3.95 \pm 0.20$ $d_1 = 2.48 \pm 0.20$	1.84	0.17
16% Na_2S-$C_2H_4(OH)_2$	–	–	–	11.0	15.00	G	$d_2 = 1.93 \pm 0.30$	1.80	0.10
16% Na_2S-C_3H_7OH	0.01	0.0026	–	11.2	1.00	G	$d_2 = 11.37 \pm 0.05$	1.45	0.13
					15	G	$d_2 = 14.46 \pm 0.20$	1.79	0.01
					30	G	$d_2 = 18.42 \pm 0.20$	1.81	0.02
16% $(NH_2)_2CS$-C_3H_7OH	0.1	0.07	$<1\cdot10^{-5}$	6.0	15.00	G	$d_2 = 2.35 \pm 0.04$	1.93	0.31
21% $(NH_4)_2S$-H_2O	3.0	2.6	1.2	9.1	0.75	C	$d_2 = 2.17 \pm 0.13$ $d_1 = 2.88 \pm 0.21$	1.16	0.02
					1.00	C	$d_2 = 5.28 \pm 0.08$ $d_1 = 4.32 \pm 0.13$	1.67	0.16
					3.00	C	$d_2 = 5.92 \pm 0.08$ $d_1 = 4.28 \pm 0.13$	1.42	0.12
					10.00	C	$d_2 = 6.82 \pm 0.19$ $d_1 = 3.95 \pm 0.06$	1.22	0.00
Models, d_1, d_2 and d_3 parameters are defined in Fig. 10.									

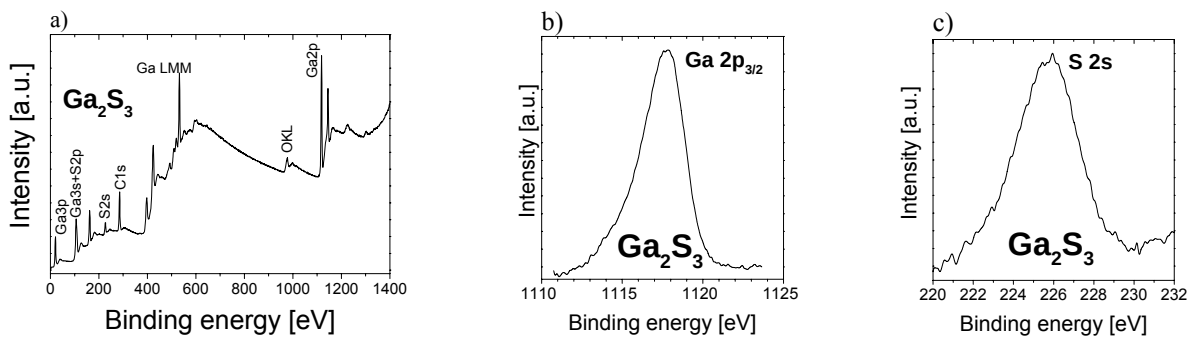

Fig. 39. XPS spectra of Ga_2S_3 standard sample: a) survey spectrum, b) spectrum of Ga $2p_{3/2}$, c) spectrum of S 2*s*.

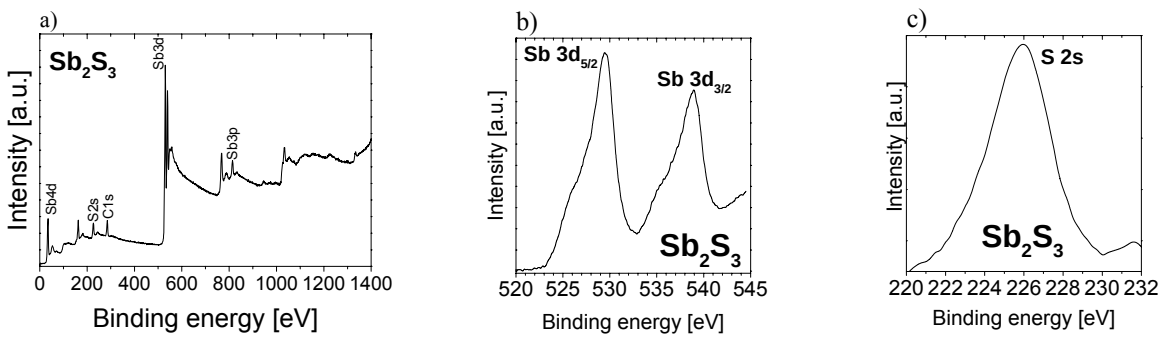

Fig. 40. XPS spectra of Sb_2S_3 standard sample: a) survey spectrum, b) spectrum of Sb $3d_{5/2}$, c) spectrum of S 2*s*.

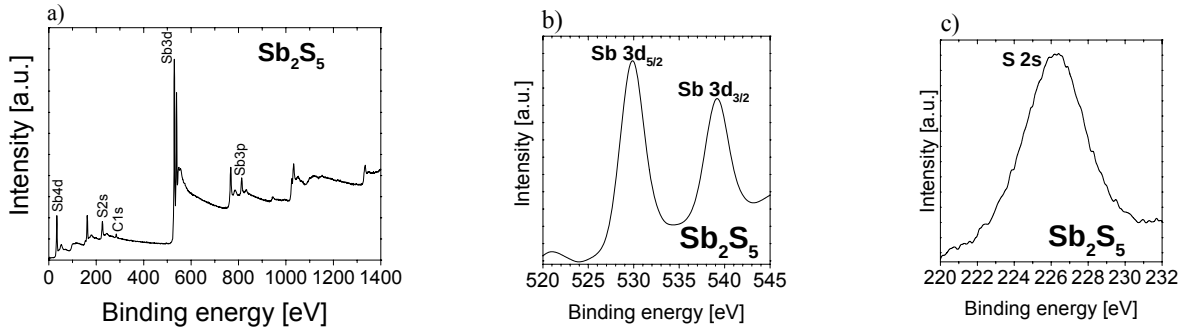

Fig. 41. XPS spectra of Sb_2S_5 model sample: a) survey spectrum, b) spectrum of Sb 3*d*, c) spectrum of S 2*s*.

There is no doubt that for times below 1 min. properties of treated surface depend more on the etching process than on passivation process itself.

Table 17. Binding energies for reference samples of Sb_2S_5, Sb_2S_3 and Ga_2S_3.

Sulphide	Spectral line	Binding energy [eV]
Sb_2S_5	Sb 3$d_{3/2}$	538.9
	Sb 3$d_{5/2}$	529.6
	S 2*s*	226.2
Sb_2S_3	Sb 3$d_{3/2}$	538.8
	Sb 3$d_{5/2}$	529.5
	S 2*s*	225.7
Ga_2S_3	Ga 2*p*	1117.8
	S 2*p*	161.4
	S 2*s*	225.8

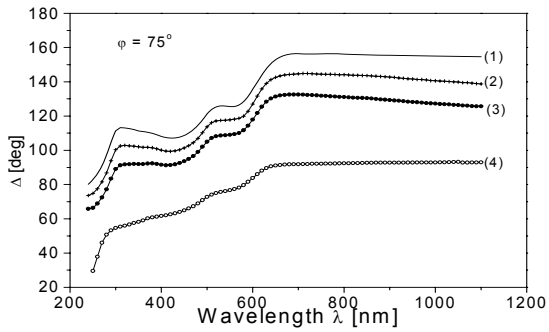

Fig. 42. Spectral characteristics Δ(λ) of (100) GaSb surface after various chemical treatments in sulphur containing solutions: (*1*) theoretical curve of GaSb surface according to J. A. Woollam Co. Inc. WVASE 32 program v 3.386, tabulated at UNL (Lincoln University, Nebraska, USA), (*2*) sulphuration in 16% Na_2S-H_2O, t = 0.75 min., @ RT, (*3*) sulphuration in 21% $(NH_4)_2S$-H_2O, t = 0.75min @ RT, (*4*) sulphuration in 16% Na_2S-C_3H_7OH, t = 0.75 min @ RT.

For longer treatment time passivation process dominates that leads to thin passivating layers. Their thickness and composition depend on other process parameters (e.g. temperature, solution pH, etc.). For example, Fig. 45 shows the XPS spectra of GaSb surface after etching in 1HCl-H_2O and passivation in 16% Na_2S - H_2O (t = 1 min.) and 16% Na_2S-C_3H_7OH (t = 1 min.). Ellipsometric (Table 16) and XPS (Fig. 45) results indicate that passivating layers formed in aqueous solutions have large oxide

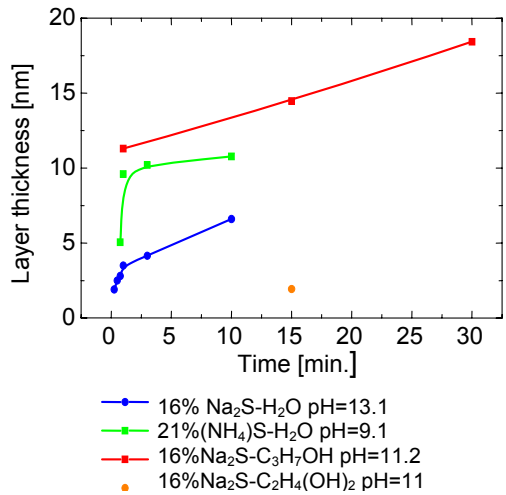

Fig. 43. Time dependence of modified surface layer thickness on sulphur passivated (100) GaSb surface.

component while passivation in alcoholic solutions allows to obtain thick coatings with a large sulphide component.

The question arises about long-term stability of sulphur-containing passivating layers. To clarify this issue the XPS spectra of (100) GaSb freshly treated in 16% Na_2S-$C_2H_4(OH)_2$ for 15 min. were compared with those of the same sample after two months long air expose. Figure 46 shows significant increase of Sb 3$d_{5/2}$ + O 1*s* signal intensity that indicates progressive reaction of passivated surface with oxygen.

To study influence of sulphur passivation on electronic properties of GaSb surface Au/n-GaSb Schottky diodes were prepared on passivated and non-passivated (100) GaSb wafers. Figure 47 shows current-voltage characteristics of such diodes, while Table 18 presents their ideality factor, height of the Schottky barrier and intensity of reverse current. As it is seen, sulphur passivation of GaSb surface leads to higher Schottky barrier, closer to one ideality factor and smaller reverse current of the diode. This illustrates significant improvement of diode characteristics being due to sulphur passivation of the GaSb surface. Similar finding has been reported by Perotin et al. [50] and Dutta et al. [51]. Thus, chemical passivation of semiconductor surface in sulphur containing solutions seems to be promising tool in device production. Since passivated surfaces are quickly covered by

additional coatings, long-term stability of passivation in air is not a big issue in this case.

Surface passivation techniques can be used to protect freshly deoxidised substrates for the time needed to load them to epitaxial reactors. For example, hydrogen passivation of silicon, obtained by final dip in diluted HF, is commonly applied prior to epitaxial growth on silicon substrates. We checked applicability of sulphur passivation of (100) GaSb substrates as surface protection prior to LPE growth of GaSb/InGaAsSb/AlGaAsSb heterostructures for photovoltaic detectors and LED operating in the mid-infrared. For passivation process both 16% Na_2SH_2O, (t = 1 min.) and 16% Na_2S-C_3H_7OH (t = 1 min.) solutions were used. After loading the substrates passivating layers were removed by vacuum annealing inside LPE reactor at T = 640°C for t = 1 h. The AFM micrographs of treated (100) GaSb surfaces shown in Fig. 48 indicate that roughness of so prepared surface does not exceed 0.4 nm.

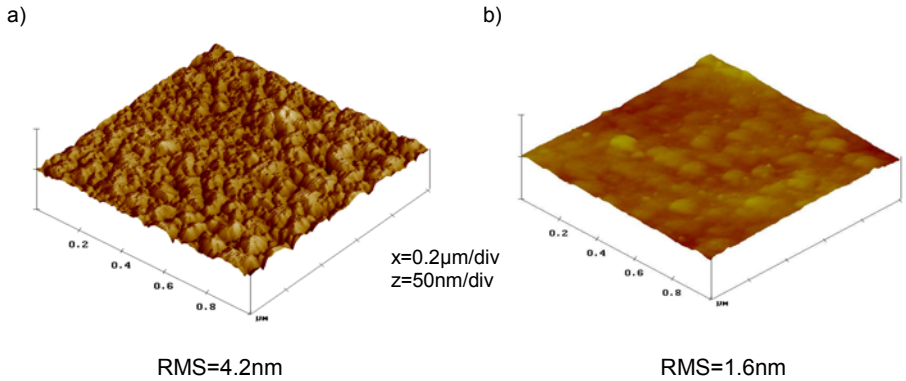

Fig. 44. AFM micrographs of (100) GaSb surface after chemical passivation in: a) 16% Na_2S-H_2O, t = 1 min. @ RT, b) 16% Na_2S-C_3H_7OH, t = 1 min. @ RT.

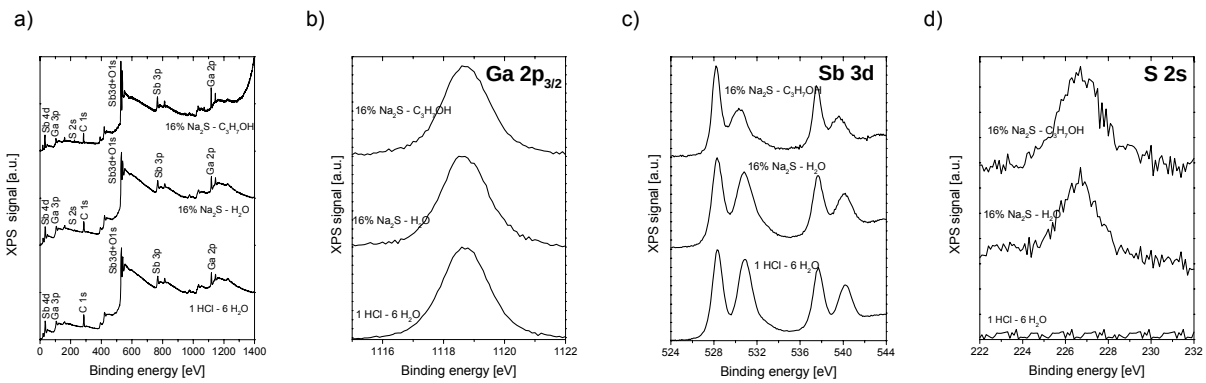

Fig. 45. XPS spectra of passivated and non-passivated (100) GaSb surface: a) survey spectrum: b) spectrum of Ga $2p_{3/2}$, c) spectrum of Sb 3d, d) spectrum of S 2s.

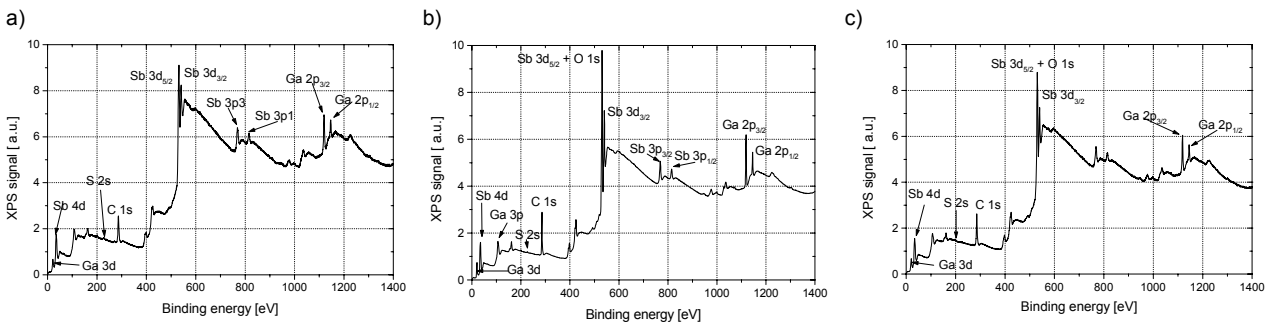

Fig. 46. XPS spectra of (100) GaSb surface passivated in 16% Na_2S-$C_2H_4(OH)_2$ measured: a) directly after passivation process, b) after 1 month of air exposure, c) after 2 months of air exposure.

Table 18. Parameters of Au/n-GaSb Schottky diodes.

Pre-treatment of GaSb surface	Ideality factor n	Height of the Schottky barrier Φ [eV]	Reverse current at U_R = 0.2 V [µA]
30HCl+1HNO$_3$ at T = 5°C, t = 0.33 min., 1HCl-6H$_2$O, t = 1 min.	1.2 ÷ 1.3	0.45	480.0
16% Na_2S - H_2O at RT, t = 10 min.	1.18	0.52	23.0
21% $(NH_4)_2S$-H_2O, at RT, t = 30 min.	1.03	0.49	50.0

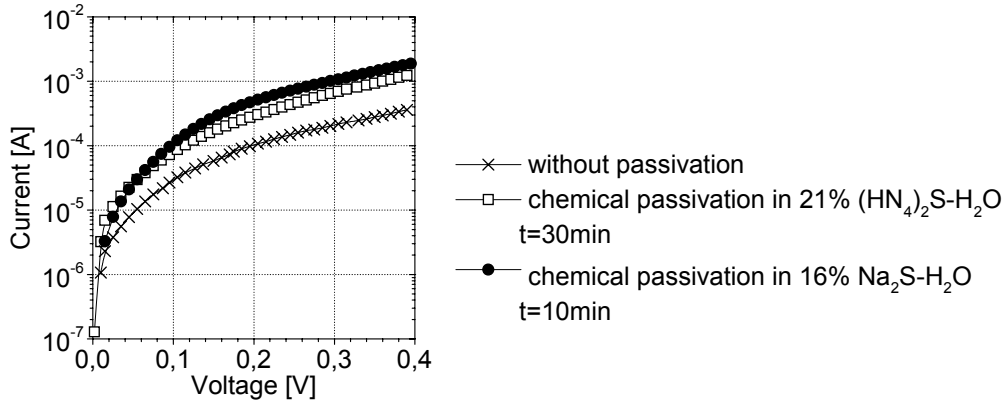

Fig. 47. Forward current-voltage characteristics of the GaSb Schottky barrier for various GaSb surface treatments.

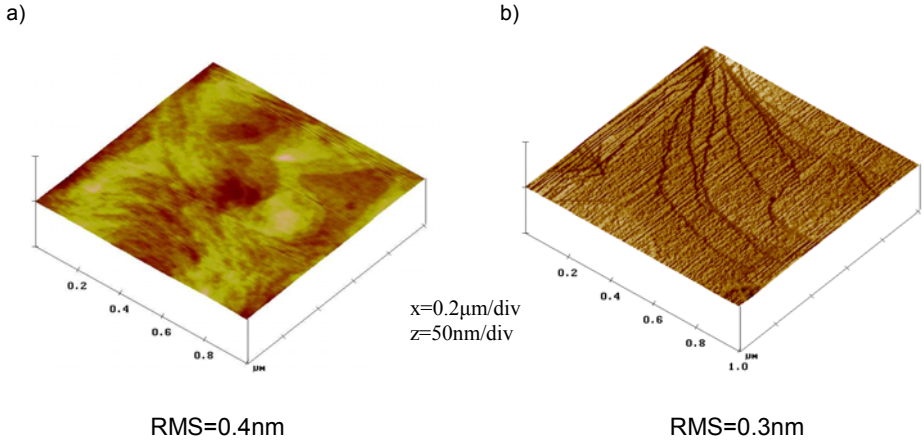

Fig. 48. AFM micrographs of (100) GaSb surface after: a)sulphuration in 16%Na_2S-H_2O, t = 1 min., annealing @T = 640°C, t = 60 min. in vacuum, b) sulphuration in w 16%Na_2S-C_3H_7OH, t = 1 min., annealing@T = 640°C, t = 60 min. in vacuum.

Sulphide treatment of GaSb substrate influences structural quality of GaSb/InGaAsSb heterostructre grown on top of it by LPE. Figure 49 shows X-ray diffraction rocking curve of InGaAsSb epilayer grown on sulphide-treated GaSb substrate. Well developed intensity oscillations testifying improved abruptness of the heterojunction are clearly visible. Also TEM micrographs shown in Fig. 50 prove better quality of GaSb/InGaAsSb interface when surface pretreatment of GaSb substrate in Na_2S followed by in situ annealing at 640°C were applied before LPE

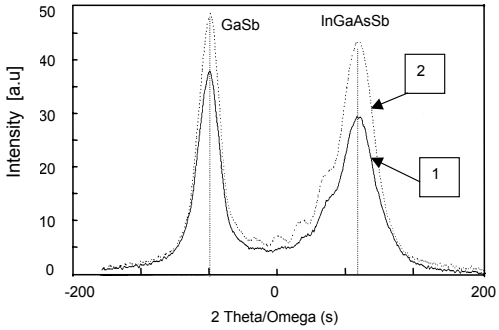

Fig. 49. X-ray diffraction spectra of $In_{0.19}Ga_{0.81}As_{0.16}Sb_{0.84}$ grown by LPE on (100) GaSb surface treated in: a) HCl-6H_2O, t = 0.33 min., b) 16%Na_2S-H_2O, t = 1 min. and annealed @T = 640°C, t = 1 min.

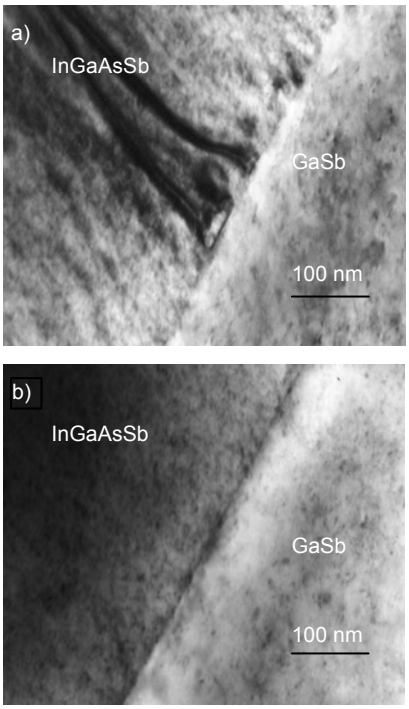

Fig. 50. Cross-sectional TEM micrographs of $In_{0.19}Ga_{0.81}As_{0.16}Sb_{0.8}$ grown by LPE on (100) GaSb surface treated in: a) HCl-6H_2O, t = 0.33 min., b) 16%Na_2S-H_2O, t = 1 min. and annealed @ T = 640°C, t = 1 min.

growth. Table 19 shows values of epilayer/substrate lattice mismatch and the carrier concentration in undoped n-type InGaAsSb epilayers. It should be point out that low doping level in n-InGaAsSb epilayers is crucial for their application in PDs structures. The results shown in Table 18 prove that good lattice matching between GaSb substrate and InGaAsSb epilayer has been obtained. Moreover, they indicate that sulphide pre-treatment reduces the carrier concentration in InGaAsSb layer to 10^{15} cm^{-3}. Most probably this results from better quality of GaSb surface after sulphurisation/annealing treatment. The presence of sulphur in the growth solution might also be beneficial for the reduction of native acceptor centres in InGaAsSb. In particular, we have found that sulphide preepitaxial treatment improves spectral characteristics of photodiodes and increases their detectivity up to $D^*_\lambda = 3\cdot10^{10} \div 2\cdot10^{11}$ cmHz$^{1/2}$/W. Moreover, we have observed a threefold increase of quantum efficiency and twofold increase of emission power for InGaAsSb/ /AlGaAsSb LEDs if our new procedure of sulphide pretreatment of (100) GaSb substrate prior to LPE growth is used. As example, Fig. 51 shows significant improvement of current-voltage characteristic of InGaAsSb/ AlGaAsSb LED made on GaSb substrate passivated in sulphur containing solution.

Table 19. Influence of (100) GaSb surface pre-treatment on carrier concentration in undoped epilayers InGaAsSb.

Epi-layer material	Pre-treatment of substrate surface		Vacuum annealing *in situ* in LPE reactor		Carrier concentration [cm^{-3}]
	Solution	t [min.]	T [°C]	t [min.]	
$In_{0.19}Ga_{0.81}As_{0.16}Sb_{0.84}$	1HCl-6H_2O	0.33	640	60	$(2.6–13)\cdot10^{16}$
	16%Na_2S-H_2O	1.00	640	60	$2.8\cdot10^{15}$
	21%$(NH_4)_2S$-H_2O	1.00	640	60	$5.1\cdot10^{15}$
$In_{0.23}Ga_{0.77}As_{0.18}Sb_{0.82}$	1HCl-6H_2O	0.33	640	60	$(2.1–20)\cdot10^{16}$
	16%Na_2S-H_2O	0.75	640	60	$4.7\cdot10^{15}$
	21%$(NH_4)_2S$-H_2O	15.0	640	60	$1.1\cdot10^{16}$

3.4.2. Electrochemical sulphuration of GaSb and related compounds

Having experience in chemical passivation of GaSb we have compared results of electrochemical sulpuration of GaSb and GaSb-based compounds using three solutions with different sulphur sources namely $(NH_4)_2S$, Na_2S or $(NH_2)_2CS$, and with different solvents (H_2O or C_3H_7OH).

Table 20 shows the results of potentiometric and iodometric analyses of the total sulphide concentration [TS] = [S_x^{2-}] + [S^{2-}], reactive sulphide concentrations [RS] = [S_x^{2-}] + [S^{2-}] + [SO_3^{2-}] and electrical conductivity δ of these three electrolytes.

Table 20. Characteristics of electrolytes and process parameters applied for electrochemical passivation of GaSb-based materials.

Electrolyte	pH	[TS]* [mol/dm^3]	[RS]** [mol/dm^3]	T [°C]	δ [Ω^{-1}m^{-1}]	Current density [mA/cm^2]	t [min.]
21% $(NH_4)_2S$-H_2O Procedure A	9.1	2.6	3.0	22	0.12	4	30
16% Na_2S-C_3H_7OH Procedure B	11.2	0.003	0.01	22	0.030	2	15
16% $(NH_2)_2CS$-C_3H_7OH+ + 0.5% 1M($C_6H_8O_7$+C_3H_7OH) Procedure C	4.8	0.07	0.1	22	0.0017	0.4	15

*[TS] = [S_x^{2-}] + [S^{2-}] – total sulphide concentration, **[RS] = [S_x^{2-}] + [S^{2-}] + [SO_3^{2-}] – reactive sulphide concentration.

Generally, sulphur compounds are not easily soluble in alcohols and their solutions exhibit low electrical conductivity. Especially for 16% $(NH_2)_2CS$-C_3H_7OH an addition of citric acid (0.5%) is necessary to improve electrochemical characteristics of the solution. 21% aqueous solution of $(NH_4)_2S$ (a commercial product) is characterised by the highest content of active sulphur and has the best electrical conductivity. In this case however, care must be taken to avoid electrolyte-aging effect.

In particular, we have found 30% decrease of active sulphur concentration [RS] after exposing the solution to atmospheric conditions.

Figure 52 shows dependence of thickness d of passivating layer fabricated on GaSb surface on current density j and processing time t for three selected sulphur containing electrolytes. It is seen that initially the thickness increases rapidly as function of the current density and processing time, then it saturates. GaSb surface treatment in 21%

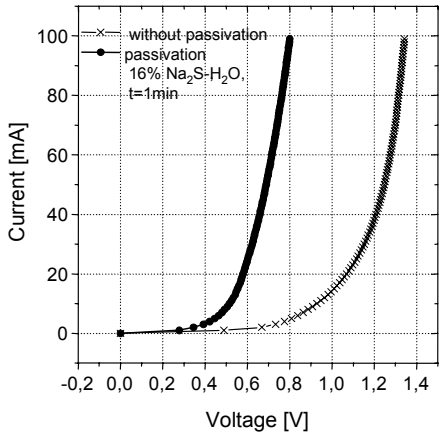

Fig. 51. Forward current-voltage characteristics of LED without passivation and after passivation of (100) GaSb substrate surface in 16%Na_2S-H_2O, t = 1 min.

aqueous solution of $(NH_4)_2S$ appears the most effective for growing thick passivating coatings. Here, the saturation of $d(j)$ curve was observed at the current density of about 35 mA/cm^2. However, in order to ensure good surface morphology the current density should be limited to j = 4 mA/cm^2.

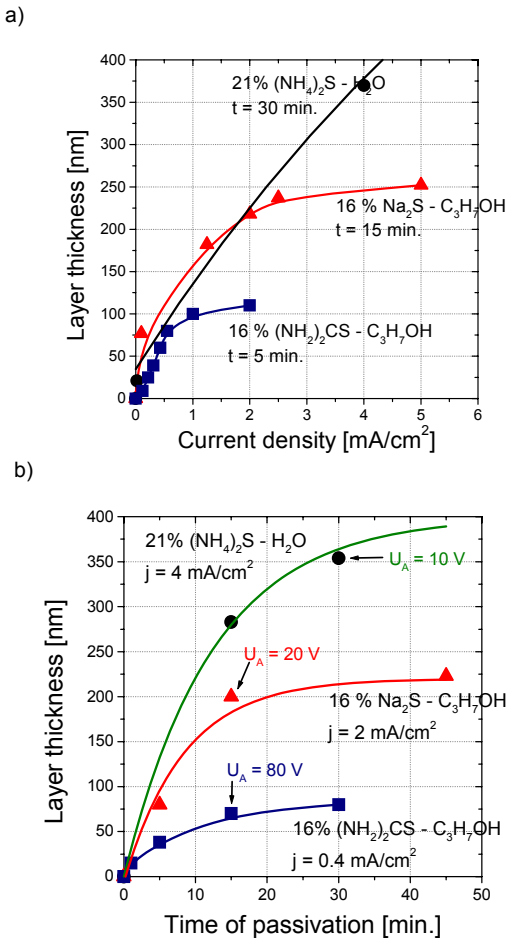

Fig. 52. The influence of the current density (a) and the processing time (b) on the thickness of passivating coating fabricated on (100) GaSb surface by electrochemical treatment in 21% $(NH_4)_2S$-H_2O, 16% Na_2S-C_3H_7OH, and 16% $(NH_2)_2CS$-C_3H_7OH solutions.

Knowing the $d(j, t)$ dependence and taking into account the results of AFM analysis (Fig. 53) we decided to concentrate on such procedures that give the thickest possible coatings with surface roughness below 10 nm. Specification of these processes is given in Table 19.

The results of studies of electrochemically sulphurated GaSb surface by XPS and spectroscopic ellipsometry are shown in Table 21. The results of VASE analyses prove insulating character of passivating coatings. In particular, Fig. 55 shows that thin films obtained by electrochemical treatment in 21% $(NH_4)_2S$ and in 16% Na_2S-C_3H_7OH exhibit good insulating properties (ε_2 = 0.014 and ε_2 = 0.029) at 1.1 eV (Fig. 54), i.e. in the wavelength region important for MIR devices. Results of peak fitting procedure for corresponding XPS spectra were compared with XPS data for unpassivated GaSb surfaces displayed in Fig. 55. The shift of Ga 2*p* signal towards higher energy, the appearance of single peaks for Sb 3*d* doublets and strong peak of S 2*s* suggest that Ga_2S_3 and Sb_2S_5 are the main components of passivating layers.

3.4.3. Electrochemical passivation of InGaAsSb and AlGaAsSb

3.4.3a. VASE analysis

Tables 22 and 23 show details of the electrochemical treatments of $In_{0.23}Ga_{77}As_{0.18}Sb_{0.82}$ and $Al_{0.34}Ga_{0.66}As_{0.025}Sb_{0.975}$ epilayers, respectively, together with thickness and complex index of refraction of the resulting thin film overcoats determined by VASE measurements. The values of optical constants are given for λ = 630 nm to allow for their comparison with the standard ellipsometric data obtained with the use of He-Ne laser.

Figure 56 shows spectral characteristics of real (n) and imaginary (k) parts of the complex index of refraction of anodic oxides grown on $In_{0.23}Ga_{77}As_{0.18}Sb_{0.82}$ and $Al_{0.34}Ga_{0.66}As_{0.025}Sb_{0.975}$ surfaces. Comparison of the VASE characteristics of anodic oxides (with various thicknesses) with those of $In_{0.23}Ga_{77}As_{0.18}Sb_{0.82}$ and $Al_{0.34}Ga_{0.66}As_{0.025}Sb_{0.975}$ surfaces after removal of anodic oxides (1HCl-6H_2O etch) allowed us to determine the optical constants of semiconductor materials under investigation. Fig. 57a shows the values of the real ε_1 and imaginary ε_2 parts of the complex dielectric function versus photon energy for $In_{0.23}Ga_{77}As_{0.18}Sb_{0.82}$ epilayer after removal of the anodic oxide. Fig. 57b displays similar data for $Al_{0.34}Ga_{0.66}As_{0.025}Sb_{0.975}$ epilayer. Ellipsometric characteristics of $\varepsilon_1(E)$ and $\varepsilon_2(E)$ obtained for $In_{0.23}Ga_{77}As_{0.18}Sb_{0.82}$ correspond well to those published by Munoz et al. [52]. No similar data has been published for $Al_{0.34}Ga_{0.66}As_{0.025}Sb_{0.975}$ so far.

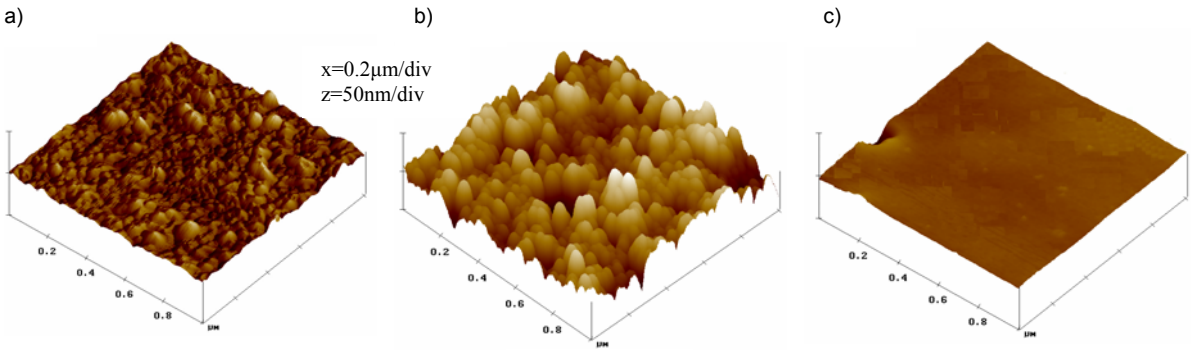

Fig. 53. AFM micrographs of (100) GaSb surface after electrochemical passivation according to procedure: A – 21% $(NH_4)_2S$-H_2O (a), B – 16% Na_2S-C_3H_7OH (b), C – 16% $(NH_2)_2CS$-C_3H_7OH (c).

Table 21. (100) GaSb surface state after electrochemical treatment in sulphur compounds solutions.

(100) GaSb surface treatment					Spectroscopic ellipsometry (for λ = 630nm)			
Procedure	Solution composition	T [°C]	Anodic voltage U_A [V]	t [min.]	Model*	Layer thickness [nm]	Refract. index n	Extinction coefficien t k
A	21% $(NH_4)_2S$ - H_2O	22	10	30	G	$d_2 = 354.20 \pm 0.02$	1.42	0.020
B	16% Na_2S - C_3H_7OH	22	20	15	G	$d_2 = 218.5 \pm 0.03$	1.53	0.004
C	16% $(NH_2)_2CS$-C_3H_7OH + 0.5% 1M ($C_6H_8O_7$+C_3H_7OH)	22	80	15	G	$d_2 = 60.18 \pm 0.10$	1.15	0.008
*Model and d_2 parameter are defined in Fig. 10.								

Table 22. Properties of (100) $In_{0.23}Ga_{0.77}As_{0.18}Sb_{0.82}$ surface layer (after electrochemical treatment.

(100) $In_{0.23}Ga_{0.77}As_{0.18}Sb_{0.82}$ surface treatment		Spectroscopic ellipsometry (for λ = 630 nm)					
Method	Solution	T [°C]	Anodic voltage U_A [V]	t [min.]	Layer thickness [nm]	Refract. index n	Extinction coefficient k
Anodic oxidation	$C_4H_6O_6$-$C_2H_4(OH)_2$ pH = 6.1	22	50	25	108.0 ± 0.1	1.95	0.08
			100	25	241.7 ± 0.1	1.95	0.08
Etching of anodic oxide	1HCl-6H_2O	22	–	1	2.00 ± 0.1	1.94	0.00
Electrochemical sulphuration	21% $(NH_4)_2S$-H_2O pH = 9.1	22	10	30	99.65 ± 0.1	1.65	0.02
Electrochemical sulphuration	16% Na_2S-C_3H_7OH pH = 13.1	22	20	15	98.00 ± 0.1	1.84	0.04

Table 23. Properties of (100) $Al_{0.34}Ga_{0.66}As_{0.125}Sb_{0.975}$ surface layer after electrochemical treatment.

(100) $In_{0.34}Ga_{0.66}As_{0.126}Sb_{0.975}$ surface treatment		Spectroscopic ellipsometry (for λ = 630 nm)					
Method	Solution	T [°C]	Anodic voltage U_A [V]	t [min.]	Layer thickness [nm]	Refractive index n	Extinction coefficient k
Anodic oxidation	$C_4H_6O_6$-$C_2H_4(OH)_2$ pH = 6.1	22	50	25	130.0 ± 0.1	1.93	0.0003
			100	25	226.5 ± 0.1	1.93	0.0003
Etching of anodic oxide	1HCl-6H_2O	22	–	1	3.00 ± 0.1	1.94	0.00
Electrochemical sulphuration	21% $(NH_4)_2S$-H_2O pH = 9.1	22	10	30	100.31 ± 0.1	1.67	0.08
Electrochemical sulphuration	16% Na_2S-C_3H_7OH pH = 13.1	22	20	15	93.00 ± 0.1	1.87	0.03

The effect of electrochemical treatment in 21% $(NH_4)_2S$-H_2O and 16% Na_2S-C_3H_7OH on the surface properties $In_{0.23}Ga_{77}As_{0.18}Sb_{0.82}$ and $Al_{0.34}Ga_{0.66}As_{0.025}Sb_{0.97}$ is illustrated in Figs. 58 and 59 where spectral characteristics $\varepsilon_1(E)$ and $\varepsilon_2(E)$ of resulting surface overcoats are shown. These prove insulating properties of both passivating coatings and their usefulness for devices operating in the near- and mid-IR wavelength ranges.

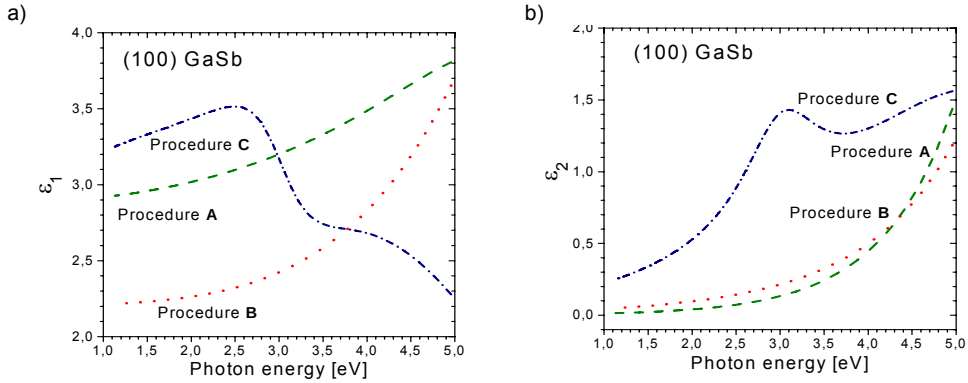

Fig. 54. Spectral characteristics of ε_1 (a) and ε_2 (b) of GaSb surface after passivation according to procedure: A – 21% $(NH_4)_2S$-H_2O, B – 16% Na_2S-C_3H_7OH and C – 16% $(NH_2)_2CS$-C_3H_7OH.

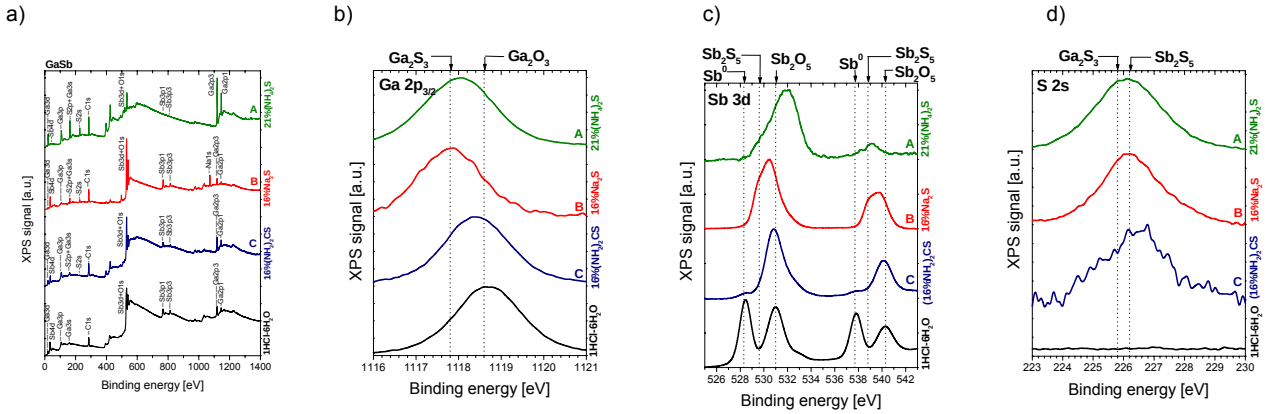

Fig. 55. XPS spectra of survey (a), Ga $2p_{3/2}$ (b), Sb 3*d* (c), and S 2*s* (d) signals from (100) GaSb surface after electrochemical treatment in 21% $(NH_4)_2S$-H_2O for 30 min., 16% Na_2S-C_3H_7OH for 15 min., and 16% $(NH_2)_2CS$-C_3H_7OH for 15 min. Data for 5% HCl treatment are shown for comparison.

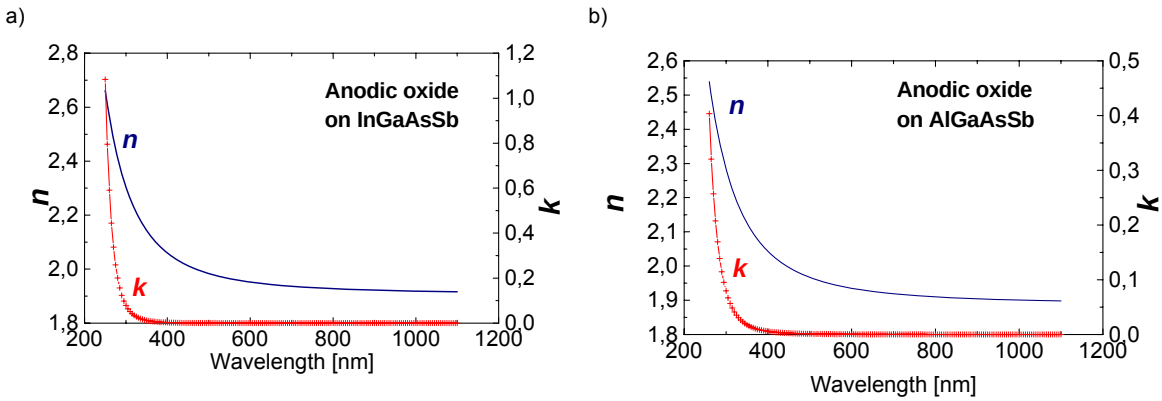

Fig. 56. Spectral characteristics $n(\lambda)$ and $k(\lambda)$ of anodic oxide (anodic oxidation in $C_4H_6O_6$-$C_2H_4(OH)_2$@ U_A = 50 V, t = 25 min.) on $In_{0.23}Ga_{77}As_{0.18}Sb_{0.82}$ (a) and $Al_{0.34}Ga_{0.66}As_{0.025}Sb_{0.975}$ (b) surfaces.

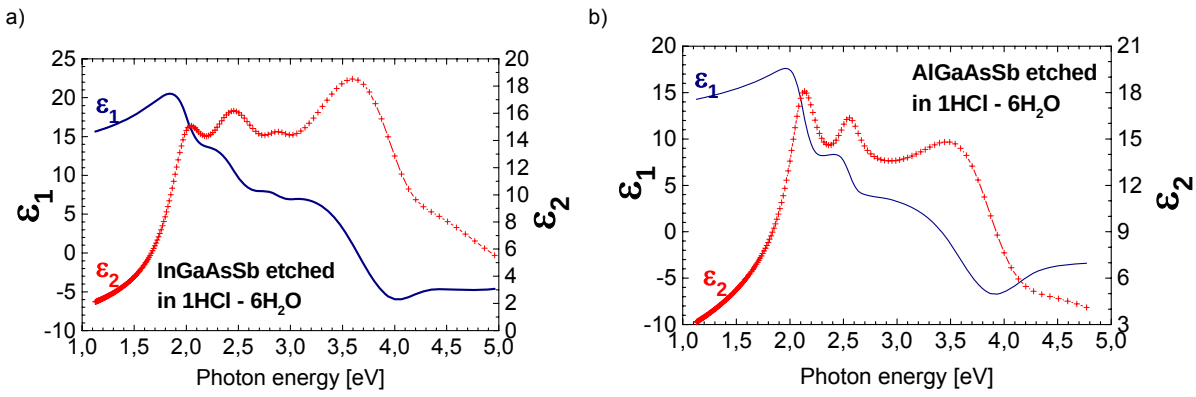

Fig. 57. Spectral characteristics $\varepsilon_1(E)$ and $\varepsilon_2(E)$ of $In_{0.23}Ga_{0.77}As_{0.18}Sb_{0.82}$ (a) and $Al_{0.34}Ga_{0.66}As_{0.025}Sb_{0.975}$ (b) surfaces.

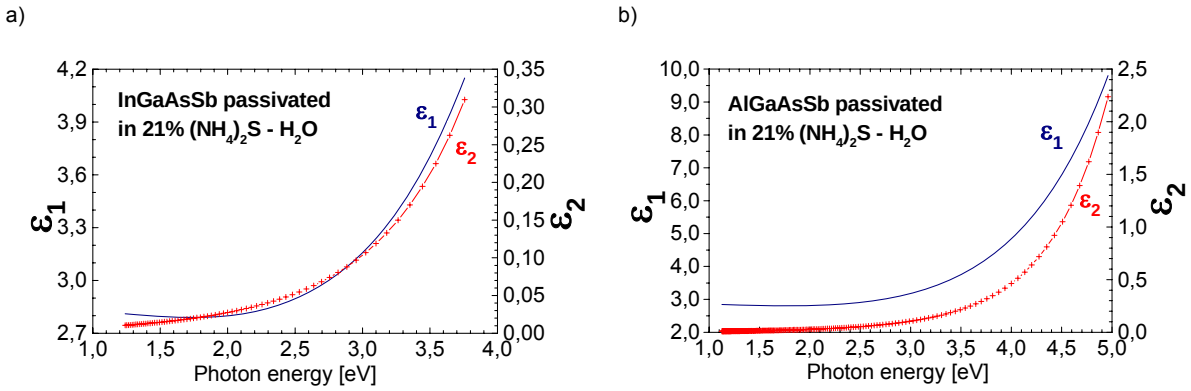

Fig. 58. Spectral characteristics $\varepsilon_1(E)$ and $\varepsilon_2(E)$ of $In_{0.23}Ga_{0.77}As_{0.18}Sb_{0.82}$ (a) and $Al_{0.34}Ga_{0.66}As_{0.025}Sb_{0.975}$ (b) surfaces passivated in 21% $(NH_4)_2S$-H_2O for 30 min.

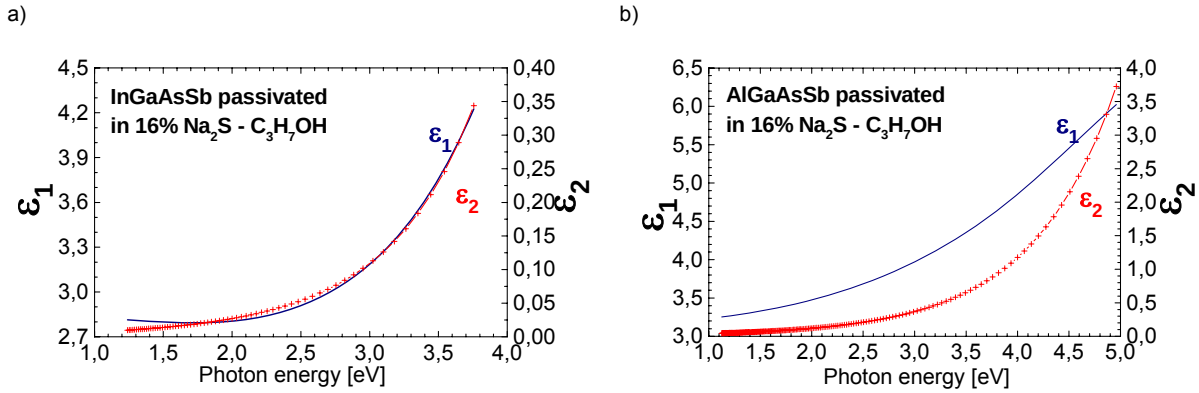

Fig. 59. Spectral characteristics $\varepsilon_1(E)$ and $\varepsilon_2(E)$ of $In_{0.23}Ga_{0.77}As_{0.18}Sb_{0.82}$ (a) and $Al_{0.34}Ga_{0.66}As_{0.025}Sb_{0.975}$ (b) surfaces passivated in 16% Na_2S-C_3H_7OH for 15 min.

3.4.3.b. X-ray photoemission

The influence of the electrochemical sulphur treatment on the composition of near-surface region of $In_{0.23}Ga_{77}As_{0.18}Sb_{0.82}$ and $Al_{0.34}Ga_{0.66}As_{0.025}Sb_{0.975}$ epilayers is illustrated in Figs. 60–62, in which XPS spectra of bare (i.e. after HCl etch only) and sulphur- -treated semiconductor samples are juxtaposed.

One of the main features distinguishing the effect of $(NH_4)_2S$-H_2O treatment from that of Na_2S-C_3H_7OH is the appearance of Na 1s line (XPS survey spectra in Fig. 60), corresponding to the formation of Na_2SO_3 on both, $In_{0.23}Ga_{77}As_{0.18}Sb_{0.82}$ and $Al_{0.34}Ga_{0.66}As_{0.025}Sb_{0.975}$ samples exposed to electrochemical treatment in Na_2S-C_3H_7OH [45]. XPS spectra of Ga $2p_{3/2}$, Sb 3*d*, S 2*s* and In 3*d* lines for $In_{0.23}Ga_{77}As_{0.18}Sb_{0.82}$ sample before sulphur treatment (i.e. after HCl etch only), namely the positions of Ga $2p_{3/2}$ spectral peak (E_B = 1118.5 eV), the Sb 3*d* doublet (E_B = 528.3 eV and E_B = 537.7 eV) and the spectral peak of In 3*d* (E_B = 442.0 eV), indicate the presence of Ga_2O_3, Sb, and In on unpassivated semiconductor surface. Arsenic signal is of too low intensity to give any informative outputs

Some features of the XPS spectra of $In_{0.23}Ga_{77}As_{0.18}Sb_{0.82}$ sample after electrochemical treatment in 21% $(NH_4)_2S$-H_2O, specifically, the shift of Ga *2p* line towards lower energy (E_B = = 1117.8 eV), the appearance of strong peaks in Sb 3*d* doublet (with binding energy E_B = 538.9 eV for Sb $3d_{3/2}$ line and E_B = 529.6 eV for Sb $3d_{5/2}$ line), and strong peak of S 2*s* (E_B = 225.9 eV) prove that Ga_2S_3 and Sb_2S_5 are the main components of passivating layer. Moreover, the appearance of strong In 3*d* line (E_B = 444.8 eV), indicate the formation of In_2S_3 in surface region. Such conclusion agrees very well with literature data [53].

XPS spectra of $In_{0.23}Ga_{77}As_{0.18}Sb_{0.82}$ sample after electrochemical treatment in 16% Na_2S-C_3H_7OH show similarities to those obtained after 21% $(NH_4)_2S$-H_2O treatment, as far as the shift of Ga $2p_{3/2}$ line towards lower energy and the appearance of Sb 3*d* and In 3*d* doublets (indicating formation of Ga_2S_3, Sb_2S_5, and In_2S_3) are concerned. However, contrary to the 21% $(NH_4)_2S$-H_2O treatment, the XPS spectrum of S 2*s* (Fig. 61c) shows two distinct peaks, which suggests that in this case sulphur exists in two chemical states. Specifically, apart from low energy peak at E_B = 225.9 eV attributed to the formation of Sb_2S_5 another peak at E_B = 233.2 eV indicates formation of additional compound. The published XPS data on binding energies of sulphur compounds are based on the analysis of S 2*p* lines. Unfortunately, since the S 2*p* spectra overlap with that of Ga 3*s* we had to analyse 3 2*s* spectra rather than of S 2*p*. Consequently, literature data for S 2*p* could not be directly applied to our analysis. However, taking into account that the distance between the two lines attributed to two

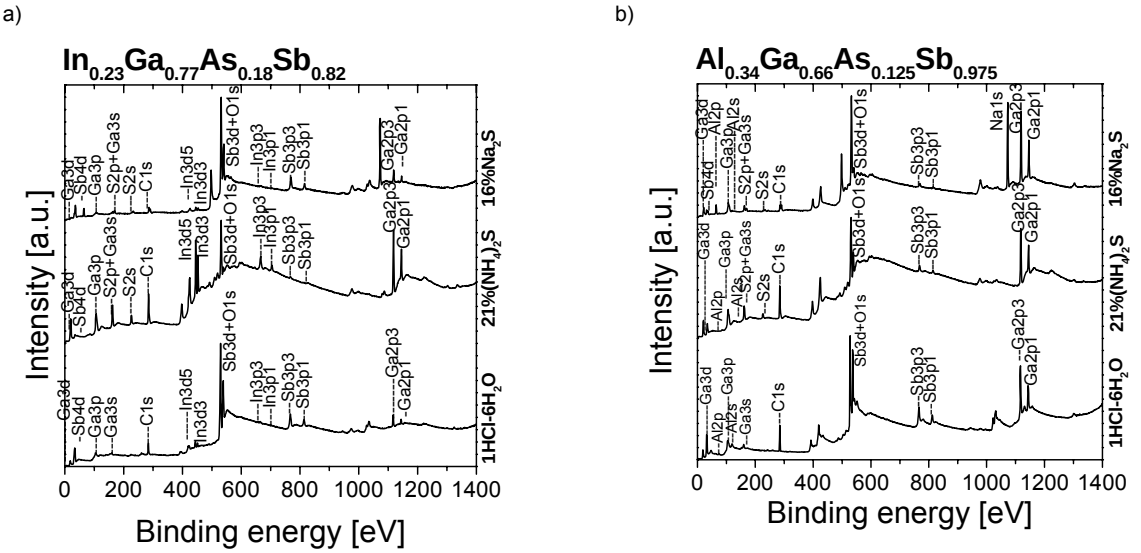

Fig. 60. XPS survey spectra of $In_{0.23}Ga_{0.77}As_{0.18}Sb_{0.82}$ (a) and $Al_{0.34}Ga_{0.66}As_{0.025}Sb_{0.975}$ (b) surface after electrochemical passivation in 21% $(NH_4)_2S$-H_2O and 16% Na_2S-C_3H_7OH. Data for 5%HCl treatment are shown for comparison.

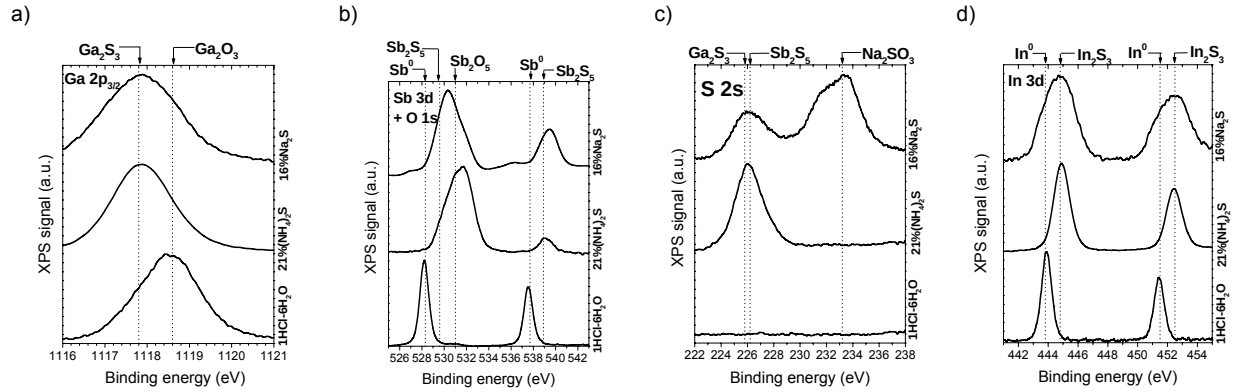

Fig. 61. XPS spectra of Ga 2$p_{3/2}$ (a), Sb 3d (b), S 2s (c) and In 3d (d) signals from $In_{0.23}Ga_{0.77}As_{0.18}Sb_{0.82}$ surface after electrochemical treatment in 16% Na_2S-C_3H_7OH and 21% $(NH_4)_2S$-H_2O. Data for 5%HCl treatment are shown for comparison.

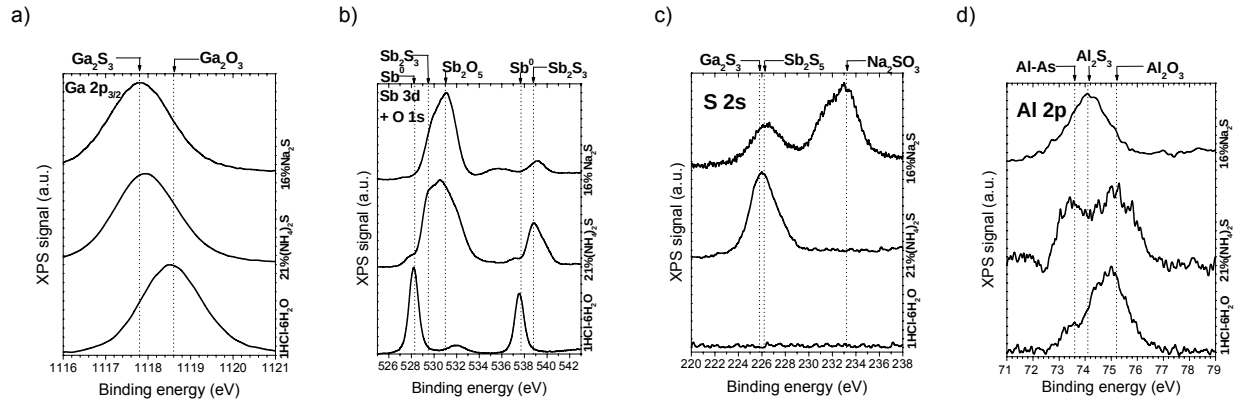

Fig. 62. XPS spectra of Ga 2$p_{3/2}$ (a) Sb 3d (b), S 2s (c) and Al 2p (d) signals from $Al_{0.34}Ga_{0.66}As_{0.025}Sb_{0.975}$ surface after electrochemical treatment 16% Na_2S-C_3H_7OH and 21% $(NH_4)_2S$-H_2O. Data for 5%HCl treatment are shown for comparison.

chemical states for S 2p spectra agrees with the distance between analogous lines for S 2s spectra, we suggest that the high energy line for S 2s spectra (E_B = 233.2 eV) can be attributed to the formation of Na_2SO_3.

XPS spectra of Ga 2$p_{3/2}$, Sb 3d, S 2s and Al 2p lines registered for $Al_{0.34}Ga_{0.66}As_{0.025}Sb_{0.975}$ samples (Fig. 62) indicate the presence of Sb, Ga_2O_3, Al_2O_3 and Al-As bonds on unpassivated surface (after HCl etch). In particular, the Al 2p line indicates two chemical states of Al. The line at binding energy of about E_B = 75 eV can be attributed to Al_2O_3 although its position is slightly shifted to higher energies in comparison to the literature data [45]. The low binding energy state can be related to the bonding of aluminium to arsenic, with agreement to the reported value of binding energy of E_B = 73.6 eV for Al-As bond [45].

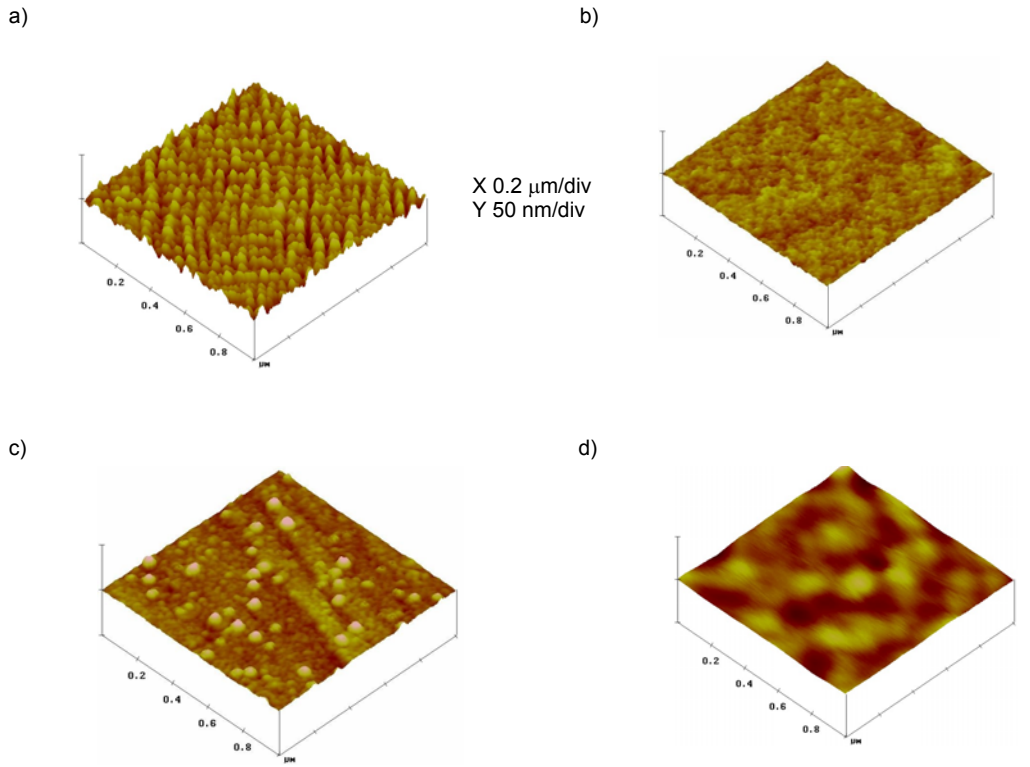

Fig. 63. AFM micrographs of $In_{0.23}Ga_{77}As_{0.18}Sb_{0.82}$ surface: a) before, b) after passivation in 21% $(NH_4)_2S$-H_2O for 30 min. and $Al_{0.34}Ga_{0.66}As_{0.025}Sb_{0.975}$ surface: c) before, d) after passivation in 21% $(NH_4)_2S$-H_2O for 30 min.

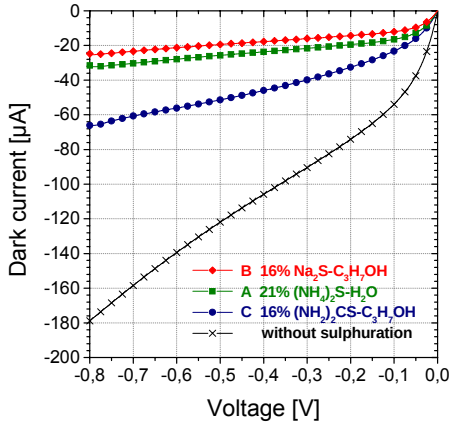

Fig. 64. The influence of electrochemical treatment in 21% $(NH_4)_2S$-H_2O for 30 min., 16% Na_2S-C_3H_7OH for 15 min., and 16% $(NH_2)_2CS$-C_3H_7OH for 15 min. on dark current of InGaAsSb/AlGaAsSb photodiodes.

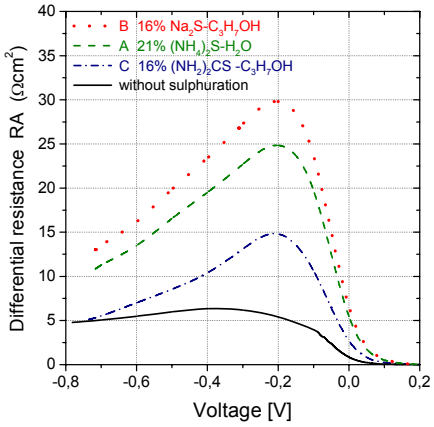

Fig. 65. The influence of electrochemical treatment in 21% $(NH_4)_2S$-H_2O for 30 min., 16% Na_2S-C_3H_7OH for 15 min., and 16% $(NH_2)_2CS$-C_3H_7OH for 15 min. on differential resistance of InGaAsSb/AlGaAsSb photodiodes.

Electrochemical treatment in 21% $(NH_4)_2S$-H_2O results in the shift of Ga $2p_{3/2}$ line (to E_B = 1117.8 eV) and the appearance of Sb 3*d* doublet, proving the presence of Ga_2S_3 and Sb_2S_5 on $Al_{0.34}Ga_{0.66}As_{0.025}Sb_{0.975}$ surface. Again, the Al 2*p* line indicates formation of Al_2O_3 and of the Al-As bonds in the surface region.

After electrochemical treatment in 16% $Na_2SC_3H_7OH$ the surface region of $Al_{0.34}Ga_{0.66}As_{0.025}Sb_{0.975}$ epilayer has a different chemical composition. Apart from spectral lines corresponding to the formation of Ga_2S_3 and Sb_2S_5, the spectrum of Al *2p* line suggests formation of Al_2S_3 while that of S 2*s* the appearance of Na_2SO_3. Additionally, AFM micrographs of (100) GaSb surface before and after passivation presented in Fig. 63 indicate that electrochemical passivation in 21% $(NH_4)_2S$-H_2O, 16% Na_2S-C_3H_7OH and 16%$(NH_2)_2CS$-C_3H_7OH allows to obtain a smooth surface with roughness below 10 nm.

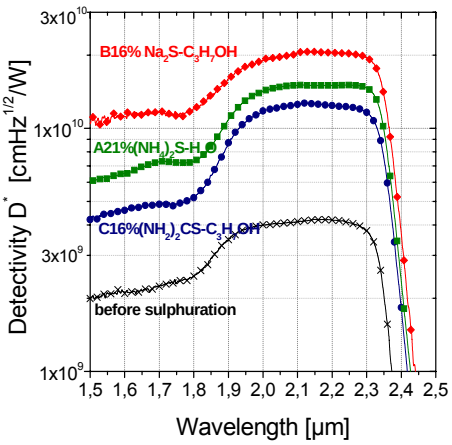

Fig. 66. The influence of electrochemical treatment in 21% $(NH_4)_2S$-H_2O for 30 min., 16% Na_2S-C_3H_7OH for 15 min., and 16% $(NH_2)_2CS$ - C_3H_7OH for 15 min. on detectivity of InGaAsSb/AlGaAsSb photodiodes.

a)

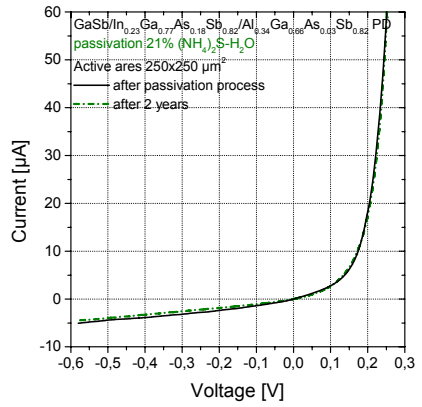

b)

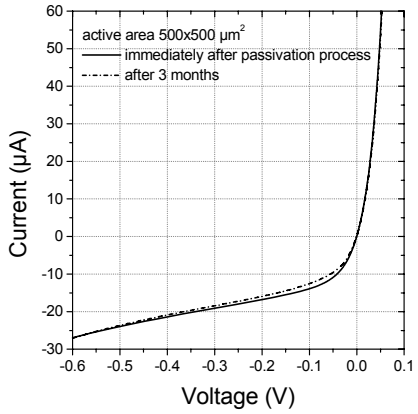

Fig. 67. Long-term stability of I(V) characteristics of InGaAsSb/AlGaAsSb PDs photodiodes passivated in 21% $(NH_4)_2S$-H_2O for 30 min. (a) and 16% Na_2S-C_3H_7OH for 15 min. (b).

The effect of electrochemical passivation of mesa side walls on the properties of GaSb/n-$In_{0.23}Ga_{77}As_{0.18}Sb_{0.82}$/p-$Al_{0.34}Ga_{0.66}As_{0.025}Sb_{0.975}$ photodiodes is illustrated in Table 24 and on Figs. 64–66. Significant improvement of photodetector parameters, i.e. lower dark current and increase of the differential resistance and of the detectivity, has been obtained when applying 21% $(NH_4)_2S$ (at pH = 9.1, $j = 4$ mA/cm^2, $t = 30$ min) or 16% Na_2S-C_3H_7OH (at pH = 11.0, $j = 2$ mA/cm^2, $t = 15$ min.) treatments. Reliability studies have been carried out for these two passivation procedures and their results are shown in Fig. 67. Ageing of photodiodes passivated in 21% $(NH_4)_2S$ was performed within 24 months, while those passivated in 16% Na_2S-C_3H_7OH is still in progress. Thus, both treatments show long term stability of the passivation effect.

Table 24. Influence of electrochemical sulphuration treatment on parameters of GaSb/n-$In_{0.23}Ga_{77}As_{0.18}Sb_{0.82}$/ /p-$Al_{0.34}Ga_{0.66}As_{0.025}Sb_{0.975}$ photodetectors.

Pro-cedure	R_o [Ω]	R_i @ 2.2 μm [A/W]	η	Noise current [pA/HZ$^{1/2}$]	D^* @ 2.2 μm [cmHz$^{1/2}$/W]
Without sulphur.	500	0.9	0.5	10	$4 \cdot 10^9$
A	1600	1.3	0.7	4	$1.5 \cdot 10^{10}$
B	2000	1.5	0.8	4	$2 \cdot 10^{10}$
C	1200	1.8	0.6	7	$1.2 \cdot 10^{10}$
R_o – differential resistance, R_i – responsibility, η –quantum efficiency, D – detectivity					

The conclusion of the experiments presented above is that both A and B procedures can be used for effective passivation of GaSb-based surfaces. Specifically, electrochemical treatment in 21% $(NH_4)_2S$ aqueous solution allows obtaining 300 nm thick sulfide coatings, while passivation in Na_2S alcoholic solution produces 100 nm thick sulfide layers. These coatings when applied for passivation of mesa side walls of GaSb/InGaAsSb/AlGaAsSb photodiodes enable reducing their dark current by a factor of 4 and increasing the differential resistance by a factor of 4. As the final result of our studies devices charac- terised by the detectivity of $1.5 \div 2 \cdot 10^{10}$ cmHz$^{1/2}$/W and dark current density of 20 mA/cm^2 at –0.5 V bias have been fabricated and their long-term stability has been proven.

4. Conclusions

Summarising, various procedures of GaSb surface chemical processing have been developed. Our studies show that for processing of optoelectronic devices the best results are obtained by (i) chemo-mechanical polishing in Br_2-ethylene glycol, (ii) pre- epitaxial treatment of GaSb substrates in Na_2S-H_2O followed by in-situ annealing in vacuum, (iii) surface treatment in 30HCl-1HNO_3 followed by 5%HCl etch prior to metal/dielectric deposition, and (iv) surface passivation in either aqueous $(NH_4)_2S$ or alcoholic Na_2S solutions. Another important result of this study is the evaluation of optical constants for $In_{0.23}Ga_{77}As_{0.18}Sb_{0.82}$ and $Al_{0.34}Ga_{0.66}As_{0.025}Sb_{0.975}$ in the mid-IR region. Such data has not been published so far. Presented XPS data of bulk Ga_2S_3, Sb_2S_3 and Sb_2S_5 samples can be used as reference in further XPS analysis of sulphurised surfaces of GaSb-based materials.

The measurable result of this work was successful application of elaborated processes for the fabrication of efficient optoelectronic devices operating in the mid-infrared wavelength range.

Acknowledgements

The author is very much indebted to Prof. A. Piotrowska and Dr E. Kaminska for their inspiration and many helpful discussions and comments on this article.

I am grateful to my colleagues and coworkers: Mrs K. Babska, Mrs K. Gołaszewska, Mrs L. Ilka, Mrs R. Kruszka, Mrs P. Mihalovits, Mrs A. Ostafin, Dr M. Guziewicz, Dr T. Piotrowski, Dr M. Piskorski, Mr Z. Szopniewski and Mr R. Łukasiewicz for their help and contribution at various stages of laboratory work.

I wish to thank Dr A. Kudła and Mr W. Rzodkiewicz for ellipsometric measurements and Prof. J. Kątcki and Dr J. Ratajczak for SEM and TEM studies of our samples.

Finally I would like to express my gratitude to Dr J. Szade and Dr A. Winiarski for XPS analysis of sulphur passivated surfaces, Prof. J. Rutkowski for electrooptic measurements, Dr J. Wróbel for his help with electrono-lithography and Dr A. Wawro and Dr M. Aleszkiewicz for AFM measurements.

This research is partially supported by the Ministry of Science and Information Society Technologies, Poland, under the grant 4T 11B 039 22.

REFERENCES

1. M. INVISHI, B. W. WESSELS, *Deep Level Transient Spectroscopy of Interface and Bulk Trap States in InP MOS Structures*, Thin Solid Films, 1983, **103**, 141.
2. C. C. CHANG, P. H. CITRIN, B. SCHWARTZ, *Chemical Preparation of GaAs Surfaces and Their Characterization by Auger Electron and X-ray Photoemission Spectroscopies* , J. Vacuum Sci. Technol., 1977, **14**, 943.
3. W. E. SPICER, I. LINDAU, P. PIANETTA, P. W. CHYE, C. M. GARNER, *Fundamental Studies of III-V, Surfaces and the (III-V)-Oxide Interface*, Thin Solid Films, 1979, **56**, 1.
4. A. J. ROSENBERG, *The Oxidation of Intermetallic Compounds III-V. The Room-Temperature Oxidation of $A^{III}B^{V}$ Compounds*, J. Phys. Chem. Solids, 1960, **14**, 175.
5. W. E. SPICER, I. LINDAU, P. SKEATH, C. Y. SU, *Unified Defect Model and Beyond*, J. Vacuum Sci. Technol., 1980, **17**, 1019.
6. H. IWASAKI, Y. MIZOKAWA, R. NISHITANI, S. NAKAMURA, *X-Ray Photoemission Study of the Initial Oxidation of the Cleaved (110) Surfaces of GaP and InSb*, Surf. Sci., 1979, **86**, 811.
7. P. W. CHYE, I. LINDAU, P. PIANETTA, C. M. GARNER, C. Y. SU, W. E. SPICER, *Photoemission Study of Au Schottky-Barrier Formation on GaSb, GaAs and InP using Synchrotron Radiation*, Phys. Rev. B, 1978, **18**, 5545.
8. E. W. KREUTZ, E. RICKUS, N. SOTNIK, *Oxidation Properties of InSb (100) Surfaces*, Surf. Sci., 1977, **68**, 392.
9. H. IWASAKI, Y. MIZOKAWA, R. NISHITANI, S. NAKAMURA, *Effects of Water Vapour and Oxygen Excitation on Oxidation of GaAs, GaP and InSb Surfaces Studied by X-Ray Photoemission Spectroscopy*, Jpn. J. Appl. Phys., 1979, **18**, 1525.
10. P. S. DUTTA, K. L. BHAT, *The Physics and Technology of Gallium Antimonide: an Emerging Optoelectronic Material*, J. Appl. Phys., 1997, **81**, 5821.
11. C. W. WILMSEN, *Physics and Chemistry of III-V Compound Semiconductor Interfaces*, Plenum Press, New York, 1985.
12. Ch. L. LIN, Y. K. SU, T. S. SE, W. L. LI, *Variety Transformation of Compound at GaSb Surface under Sulfur Passivation*, Jpn. J. Appl. Phys., 1998, **37**, 1543.
13. B. STEPANEK, V. SESTAKOVA, *Indium and Nitrogen Doping of GaSb Single Crystal*, J. Crystal Growth, 1992, **123**, 306.
14. M. KODAMA, J. HASEGAWA, M. KIMATA, *Influence of Substrate Preparation on the Morphology of GaSb Films Grown by Molecular Beam Epitaxy*, J. Electrochem. Soc., 1985, **132** (3), 659.
15. W. FAUST, A. SAGAR, *Effect of the Polarity of the III-V Intermetallic Compounds on Etching* J. Appl. Phys., 1960, **31**, 331.
16. M. KODAMA, *Improvement of Reverse Leakage Current Characteristics of GaSb and $Al_{0.3}Ga_{0.7}As$/GaSb Diodes Grown by MBE*, Solid-State Electron, 1994, **37**(8), 1567.
17. J. D. VENABLES, R. M. BROUDY, *Dislocations and Selective Etch Pits in InSb*, J. Appl. Phys., 1958, **29** (7), 1025.
18. H. C. GATOS, M. C. LAVINE, *Characteristics of the (111) Surfaces of the III-V Intermetallic Compounds*, J. Electrochem. Soc., 1960, **107**, 427.
19. R. E. MARINGER, *Etch Pitting on Single-Crystal InSb*, J. Appl. Phys., 1958, **29**, 1261.
20. F. D. AURET, *An AES Evaluation of Cleaning and Etching Methods for InSb*, J. Electrochem. Soc., 1982, **129** (12), 2752.
21. H. C. GATOS, M. C. LAVINE, *Etching Behavior of the (100) Surfaces of InSb*, J. Electrochem. Soc., 1960, **107**, 433.
22. A. HERCOG, R. R. HABERECHT, A. E. MIDDLETON, *Preparation and Properties of AlSb*, J. Electrochem. Soc., 1958, **105**, 533.
23. S. J. PEARTON, W. S. HABSON, F. A. BALOCCHI, *Reactive Ion Etching of InAs, InSb, and GaSb n CCl_2F_2/O_2 and C_2H_6/H_2*, J. Electrochem. Soc., 1990, **137**, 1924.
24. J. WERKING, J. SCHRAMM, C. NGUYEN, E. L. HU, H. KROEMER, *Methane/Hydrogen-Based Reactive Ion Etching of InAs, InP, GaAs and GaSb*, Appl. Phys. Lett., 1991, **58**, 2003.
25. S. S. OU, *Reactive ion Etching of GaSb and GaAlSb using $SiCl_4$*, J .Vacuum Sci. Technol. B, 1996, **14**, 3226.
26. A. R. GIEHL, M. KESSLER, A. GROSSE, N. HERHAMMER, H. FOUCKHART, *Deep Reactive Ion Etching of GaSb in Cl_2/Ar-Plasma Discharges Using Single-Layer Soft Mask Technologies*, J. Micromech. Microeng., 2003, **13**, 238.
27. G. M. PEAKE, R. J. SHUL, I. H. ASHBY, J. G. CEDERBERG, M. J. HAFICH, R. M. BIEFEJD, M. N. PALMISIANO, *Induc- tively Coupled Plasma Reactive Ion Etching of GaInAsSb and AlGaAsSb for Quaternary Antimonide Multiple Interconnected Module Thermophotovoltaics*, J. Vacuum Sci. Technol. B, 2003, **21** (2), 843.
28. A. R. GIEHL, M. GUMBEL, M. KESSLER, N. HERHAMMER, G. HOFFMANN, H. FOUCKHARDT, *Deep Dry Etching of GaAs and GaSb Using Cl_2/Ar Plasma Discharges,* J. Vacuum Sci. Technol. B, 2003, **21**(6), 2393.
29. S. J. PEARTON, C. R. ABERNATHY, R. F. KOPF, F. REN, *Low Temperature Chlorine-Based Dry Etching of III-V Semiconductors,* J. Electrochem. Soc., 1994, **141**, 2250.
30. S. J. PEARTON, C. R. ABERNATHY, F. REN, *High Density, Low Temperature Dry Etching in GaAs and InP Device Technology*, J. Vacuum Sci. Technol. A, 1995, **13** (3), 849,
31. G. NAGY, R. U. AHMAD, M. LEVY, R. M. OSGOOD, M. J. MANFRA, G. W. TURNER, *Chemically Assisted Ion Beam Etching of Submicron Features in GaSb*, Appl. Phys. Lett., 1998, **72** (12), 1350.

32. J. F. DEWALD, *The Kinetics and Mechanism of Formation of Anode Films on Single Crystal InSb*, J. Electrochem. Soc., 1957, **104**, 244.
33. H. C. GORTON, *Etchants for III-V Compounds, Battelle Memorial Institute Technical Publications 6,* June 1, 1958.
34. H. J. BILZ, G. LEONHARDT, G. KUNN, K. LOSCHKE, A. MEISEL, *ESCA-Untersuchngen an anodisch oxydierten 3-5 Verbindungen*, Krist. Technik, 1978, **13**, 363.
35. J. F. DEWALD, *The Kinetics and Mechanism of the Formation of Anodic Films at High Fields*, J. Eletrochem. Soc., 1955, **102**, 1.
36. J. F. DEWALD, *A Theory of the Kinetics of Formation of Anodic Films on Single Crystal InSb*, J. Eletrochem. Soc., 1957, **104**, 244.
37. C. W. WILMSEN, *Correlation Between the Composition Profile and Electrical Conductivity of the Thermal and Anodic Oxides of InSb*, J. Vacuum Sci. Technol., 1976, **13**, 64.
38. D. A. BAGLEE, D. K. FERRY, C. W. WILMSEN, H. H. WIEDER, *Inversion Layer Transport and Properties of Oxides on InAs,* J. Vacuum Sci. Technol., 1980, **17**, 1032.
39. D. A. BAGLEE, D. H. LAUGHLIN, C. W. WILMSEN, D. K. FERRY, *The Physics of MOS Insulators* (G. Lucovsky, S. T. Pantelides, F. L. Galeerner, eds.), Pergamon Press, New York, 1980.
40. V. N. BESSOLOV, M. V. LEBEDEV, E. B. NOVIKOV, B. V. TSARENKOV, *Sulfide Passivation of III-V Semiduc- ctors: Kinetics of the Photoelectrochemical Reaction*, J. Vacuum Sci. Technol. B, 1993, **11** (1), 10.
41. M. S. CARPENTER, M. R. MELLOCH, B. C. COWANS, Z. DARDAS, W. N. DELGAS, *Investigations of Ammonium Sulfide Surface Treatments on GaAs,* J. Vac. Sci. Technol. B, 1989**,** **7**, 845.
42. J. SANDROFF, M. S. HEGDE, C. C. CHANG, *Structure and Stability of Passivating Arsenic Sulfide Phase on GaAs Surfaces*, J. Vac. Sci. Technol. B, 1989, **7**, 841.
43. V. H. BESSOLOV, M. V. LEBEDEV, *Semiconductors 32, 11, 1141, 1998 Chalcogenide Passivation of III-V Semiconductor Surfaces, Semiconductors*, Semiconductors, 1998, **11**, 1141.
44. T. T. PIOTROWSKI, A. PIOTROWSKA, E. KAMINSKA, M. PISKORSKI, E. PAPIS, K. GOLASZEWSKA, J. KĄTCKI, J. ADAMCZEWSKA, A. WAWRO, J. PIOTROWSKI, Z. ORMAN, J. PAWLUCZYK, Z. NOWAK J. RATAJCZAK, *Design and Fabrication of GaSb/InGaAsSb/AlGaAsSb Mid-Infrared Photodetectors,* Optoelectron. Rev., 2001, **9** (2) 188.
45. J. F. MOULDR, W.F. STICKLE, P. E. SOBOL, K. D. BOMBEN, *Handbook of X-Ray Photoelectron Spectroscopy*, Physical Electronics, 1995.
46. H. G. TOMPKINS, W. A. MCGAHAN, *Spectroscopic Ellipsometry and Reflectometry. A User's Guide*, John Wiley & Sons, New York, 1999.
47. D. E. ASPNES, B. SCHWARTZ, A. A. STUDNA, L. DERICK, L. A. KOSZI, *Optical Properties of Anodically Grown Native Oxides on Some Ga-V Compounds from 1.5 to 6.0 eV*, J. Appl. Phys., 1977, **48** (8), 3510.
48. M. MUNOZ, K. WEI, F. H. POLLAK, *Spectral Ellipsometry of GaSb: Experimental and Modelling*, Phys. Rev. B, 1999, **60**, 8105.
49. S. OSAKABE, S. ADACHI, *Study of GaAs (001) Surfaces Treated in AQUEOUs HCl Solution*, Jpn. J. Appl. Phys., 1997, **36**, 7119.
50. M. PEROTIN, P. COUSCOV, H. LUQUET, *Passivation of GaSb by Sulphur Treatment*, J. Electron. Mater., 1994, **23**, 7.
51. P. S. DUTTA, K. S. SANGUNI, H. L. BHAT, *Sulphur Passivation of Gallium Antimonide Surfaces*, Appl. Phys. Lett., 1994, **65**, 1695.
52. M. MUNOZ, K. WEI, H. POLLAK, *Optical Constants of* $Ga_{1-x}In_xAs_ySb_{1-y}$ *Lattice-Matched to GaSb (001); Experiment and Modelling*, J. Appl. Phys., 2000, **87**, 1780.
53. J. V. LI, S. L. CHUANG, O. V. SULIMA, J. A, COX, *Passivation of AlGaAsSb/InGaAsSb/GaSb Photodiodes Using Aqueous* $(NH_4)_2S$ *Solution and Polyimide Encapsulation.* J. Appl. Phys., 2005, **97**, 104506.